

1 **Nitrogen demand, availability, and acquisition strategy control plant responses to elevated
2 CO₂**

3 **Running head:** Nitrogen demand and availability control plant responses to elevated CO₂

4 Evan A. Perkowski^{1,*}, Ezinwanne Ezekannagha¹, Nicholas G. Smith¹

5 ¹Department of Biological Sciences, Texas Tech University, Lubbock, TX

6

7 *Corresponding author:

8 2901 Main St., Lubbock, TX, 79409

9 Email: evan.a.perkowski@ttu.edu

10

11 **ORCIDs**

12 Evan A. Perkowski (0000-0002-9523-8892)

13 Ezinwanne Ezekannagha (0000-0001-7469-949X)

14 Nicholas G. Smith (0000-0001-7048-4387)

15

16 Total word count: 8034 (5350 words excluding Methods)

17 - Introduction: 1512

18 - Methods: 2684

19 - Results: 1088

20 - Discussion: 2750

21 Tables: 3

22 Figures: 4

23 Supporting Information: 9 tables, 7 figures

24 **Highlight**
25 Leaf nitrogen demand drove photosynthetic responses to elevated CO₂ independent of nitrogen
26 fertilization. Nitrogen fertilization enhanced whole-plant responses to elevated CO₂. Symbiotic
27 nitrogen fixation did not modify plant responses to elevated CO₂.

28

29 **Abstract**
30 Plants respond to increasing atmospheric CO₂ concentrations by reducing leaf nitrogen content
31 and photosynthetic capacity – patterns that correspond with increased net photosynthesis and
32 growth. Despite the longstanding notion that nitrogen availability regulates these responses, eco-
33 evolutionary optimality theory posits that leaf-level responses to elevated CO₂ are driven by leaf
34 nitrogen demand for building and maintaining photosynthetic enzymes and are independent of
35 nitrogen availability. In this study, we examined leaf and whole-plant responses of *Glycine max*
36 L. (Merr) subjected to full-factorial combinations of two CO₂, two inoculation, and nine nitrogen
37 fertilization treatments. Nitrogen fertilization and inoculation did not alter leaf photosynthetic
38 responses to elevated CO₂. Instead, elevated CO₂ decreased the maximum rate of Rubisco
39 carboxylation more strongly than it decreased the maximum rate of electron transport for RuBP
40 regeneration, increasing net photosynthesis by allowing rate-limiting steps to approach optimal
41 coordination. Increasing fertilization enhanced positive whole-plant responses to elevated CO₂
42 due to increased belowground carbon allocation and nitrogen uptake. Inoculation with nitrogen-
43 fixing bacteria did not influence plant responses to elevated CO₂. These results reconcile the role
44 of nitrogen availability on plant responses to elevated CO₂, showing that leaf photosynthetic
45 responses are regulated by leaf nitrogen demand while whole-plant responses are constrained by
46 nitrogen availability.

47

48 **Keywords**

49 acclimation, biomass, eco-evolutionary optimality, growth chamber, least-cost theory, optimal
50 coordination, photosynthesis, plant functional ecology, resource optimization

51

52 **Introduction**

53 Complex carbon and nitrogen cycles regulate terrestrial ecosystems. Terrestrial biosphere models
54 that incorporate coupled carbon and nitrogen cycles must accurately represent the processes and
55 interactions governing these cycles across different environmental scenarios to simulate carbon
56 and nitrogen fluxes reliably (Hungate *et al.*, 2003; Prentice *et al.*, 2015; Davies-Barnard *et al.*,
57 2020; Kou-Giesbrecht *et al.*, 2023). However, uncertainties remain regarding how nitrogen
58 availability and acquisition strategy influences leaf- and whole-plant responses to increasing
59 atmospheric CO₂ concentrations, leading to divergent predictions of future carbon and nitrogen
60 pools and fluxes across models (Arora *et al.*, 2020; Davies-Barnard *et al.*, 2020, 2022; Meyerholt
61 *et al.*, 2020; Stocker *et al.*, 2025).

62 Research spanning several decades has documented consistent trends in leaf and whole-
63 plant responses to elevated CO₂. At the leaf level, C₃ plants commonly exhibit increased net
64 photosynthesis rates that correspond with reduced leaf nitrogen content, stomatal conductance,
65 and photosynthetic capacity when grown under elevated CO₂ compared to ambient conditions
66 (Curtis, 1996; Drake *et al.*, 1997; Nakano *et al.*, 1997; Medlyn *et al.*, 1999; Ainsworth *et al.*,
67 2002; Ainsworth and Long, 2005; Bernacchi *et al.*, 2005; Ainsworth and Rogers, 2007; Crous *et*
68 *al.*, 2010; Lee *et al.*, 2011; Pastore *et al.*, 2019; Poorter *et al.*, 2022; Cui *et al.*, 2023; Stocker *et*
69 *al.*, 2025). At the whole-plant level, CO₂ enrichment increases total leaf area, promoting greater

70 primary productivity and biomass accumulation (Coleman *et al.*, 1993; Makino *et al.*, 1997;
71 Ainsworth *et al.*, 2002; Ainsworth and Rogers, 2007; Finzi *et al.*, 2007; Poorter *et al.*, 2022).
72 Some studies suggest that elevated CO₂ increases belowground carbon allocation and root:shoot
73 ratios (Iversen *et al.*, 2008; Iversen, 2010; Nie *et al.*, 2013; Stocker *et al.*, 2025), although these
74 responses are not consistently observed (Luo *et al.*, 1994; Poorter *et al.*, 2022) and are highly
75 variable across experiments (Stocker *et al.*, 2025).

76 Two hypotheses – the nitrogen limitation hypothesis and the eco-evolutionary hypothesis
77 – offer contrasting views on how nitrogen availability shapes plant responses to elevated CO₂.
78 The nitrogen limitation hypothesis posits that nitrogen availability constrains plant responses to
79 elevated CO₂, as nitrogen availability often limits net primary productivity and influences the
80 magnitude of the terrestrial carbon sink (Vitousek and Howarth, 1991; LeBauer and Treseder,
81 2008; Sigurdsson *et al.*, 2013; Wieder *et al.*, 2015). Elevated CO₂ increases whole-plant nitrogen
82 demand for building new tissues, which may lead to greater nitrogen limitation of net primary
83 productivity without additional ecosystem nitrogen inputs (Luo *et al.*, 2004). Thus, increased
84 nitrogen availability should amplify the positive effects of elevated CO₂ on net primary
85 productivity and biomass accumulation, provided that nitrogen availability exceeds whole-plant
86 demand. Free-air CO₂ enrichment studies offer mixed support for this hypothesis, with some
87 studies supporting its predictions (Reich *et al.*, 2006; Norby *et al.*, 2010) and others not (Finzi *et*
88 *al.*, 2006; Moore *et al.*, 2006; Liang *et al.*, 2016). The hypothesis also implies that reductions in
89 leaf nitrogen content and photosynthetic capacity under elevated CO₂ are linked to ecosystem
90 nitrogen limitation, as positive correlations between soil nitrogen availability, leaf nitrogen
91 content, and photosynthetic capacity are commonly observed (Field and Mooney, 1986; Evans,
92 1989). However, evidence shows that reductions in leaf nitrogen content and photosynthetic

93 capacity under elevated CO₂ are often decoupled from changes in nitrogen availability (Crous *et*
94 *al.*, 2010; Lee *et al.*, 2011; Pastore *et al.*, 2019), indicating that other factors, such as demand for
95 building and maintaining photosynthetic tissues, might play a more important role in determining
96 leaf-level responses.

97 Conversely, the eco-evolutionary optimality hypothesis asserts that leaf-level demand to
98 build and maintain photosynthetic enzymes drives leaf-level photosynthetic responses to elevated
99 CO₂ and that nitrogen availability does not modify these responses (Harrison *et al.*, 2021). The
100 hypothesis combines photosynthetic least-cost (Wright *et al.*, 2003; Prentice *et al.*, 2014) and
101 optimal coordination (Chen *et al.*, 1993; Maire *et al.*, 2012) theories, suggesting that elevated
102 CO₂ downregulates the maximum rate of Ribulose-1,5-bisphosphate (RuBP) carboxylase/
103 oxygenase (Rubisco) carboxylation (V_{cmax}) more strongly than the maximum rate of electron
104 transport for RuBP regeneration (J_{max}). The downregulation in V_{cmax} is attributed to increased
105 CO₂ availability under elevated CO₂, which enhances Rubisco affinity for carboxylation relative
106 to oxygenation and reduces nitrogen demand for building and maintaining additional Rubisco
107 enzymes (Bazzaz, 1990; Dong *et al.*, 2022). The eco-evolutionary optimality hypothesis predicts
108 that plants optimize leaf nitrogen allocation to photosynthetic capacity to use available light
109 efficiently while avoiding over-investment in Rubisco, which has high nitrogen and energetic
110 costs to build and maintain (Evans, 1989; Sage, 1994; Evans and Clarke, 2019). This strategy
111 enhances photosynthetic nitrogen-use efficiency and allows increased net photosynthesis rates to
112 be achieved by increasing the co-limitation of net photosynthesis rates by Rubisco carboxylation
113 and electron transport for RuBP regeneration (Chen *et al.*, 1993; Maire *et al.*, 2012; Wang *et al.*,
114 2017; Smith *et al.*, 2019). Empirical evidence supports this hypothesis (Crous *et al.*, 2010; Lee *et*
115 *al.*, 2011; Smith and Keenan, 2020; Harrison *et al.*, 2021; Dong *et al.*, 2022; Cui *et al.*, 2023),

116 though few studies have connected these patterns with concurrently measured whole-plant
117 responses.

118 While the eco-evolutionary optimality hypothesis predicts that leaf-level photosynthetic
119 responses are independent of nitrogen availability, it acknowledges that nitrogen availability
120 likely regulates whole-plant responses to elevated CO₂. The hypothesis suggests that the optimal
121 whole-plant response to elevated CO₂ involves allocating surplus nitrogen not needed to satisfy
122 leaf-level demand to build and maintain photosynthetic enzymes toward constructing additional
123 optimally coordinated leaves and other plant organs. Furthermore, the hypothesis implies that
124 optimal resource allocation to photosynthetic capacity leads to nitrogen-savings at the leaf-level,
125 which maximizes resource allocation to support whole-plant growth (Smith *et al.*, 2024). Thus,
126 the extent to which plant responses to elevated CO₂ align with the nitrogen limitation or eco-
127 evolutionary optimality hypothesis may be a question of scale, with leaf-level responses
128 influenced by leaf-level demand to build and maintain photosynthetic enzymes and whole-plant
129 responses regulated by nitrogen availability.

130 Nitrogen acquisition strategy complicates the role of nitrogen availability on plant
131 responses to elevated CO₂. Plants use a variety of strategies to acquire nitrogen, including direct
132 uptake from the soil or through symbiotic relationships with mycorrhizal fungi and nitrogen-
133 fixing bacteria (Barber, 1962; Gutschick, 1981; Smith and Read, 2008). The carbon costs
134 associated with nitrogen acquisition vary among species with different acquisition strategies and
135 depend on environmental factors such as atmospheric CO₂, temperature, light availability, and
136 nutrient availability (Fisher *et al.*, 2010; Brzostek *et al.*, 2014; Terrer *et al.*, 2018; Allen *et al.*,
137 2020; Perkowski *et al.*, 2021, 2024; Lu *et al.*, 2022; Peng *et al.*, 2023). Carbon costs to acquire
138 nitrogen can influence nitrogen uptake and, in turn, affect nitrogen allocation to different plant

139 organs, investment in photosynthetic tissues, and biomass accumulation (Terrer *et al.*, 2018;
140 Perkowski *et al.*, 2021, 2024; Waring *et al.*, 2023). Therefore, considering nitrogen acquisition
141 strategy is important when examining plant responses to elevated CO₂ across nitrogen
142 availability gradients, especially because whole-plant responses to elevated CO₂ are often
143 positively correlated with nitrogen uptake (Feng *et al.*, 2015; Stocker *et al.*, 2025). However, few
144 studies account for acquisition strategy when considering the role of nitrogen availability on
145 plant responses to elevated CO₂ (Terrer *et al.*, 2016, 2018; Smith and Keenan, 2020). Despite
146 this, emerging evidence suggests that acquisition strategies with lower carbon costs for nitrogen
147 acquisition may mitigate nitrogen limitation at the whole-plant level, though leaf-level responses
148 remain less clear (Terrer *et al.*, 2018; Smith and Keenan, 2020).

149 Here, we examined whether plant responses to elevated CO₂ align with the nitrogen
150 limitation or eco-evolutionary optimality hypothesis and assessed how nitrogen acquisition
151 strategy modifies these responses. Using a growth chamber experiment, we grew *Glycine max* L.
152 (Merr.) seedlings under two CO₂ concentrations (420, 1000 ppm CO₂), two nitrogen acquisition
153 strategies (with and without *Bradyrhizobium japonicum*), and nine soil nitrogen fertilization
154 treatments (ranging from 0 to 630 ppm N) in a full-factorial design. Inoculation with *B.*
155 *japonicum* simulated whether plants could acquire nitrogen through associations with symbiotic
156 nitrogen-fixing bacteria. We used this experimental setup to test the following hypotheses:
157 (1) Leaf photosynthetic responses to elevated CO₂ will be independent of nitrogen
158 fertilization and inoculation treatment. Instead, elevated CO₂ will decrease V_{cmax} more
159 than J_{max} , increasing the ratio of J_{max} to V_{cmax} . This response will increase net
160 photosynthesis rates under growth CO₂ conditions by allowing rate-limiting steps to
161 approach optimal coordination while enhancing photosynthetic nitrogen-use efficiency.

162 (2) Following the nitrogen limitation hypothesis, increasing nitrogen fertilization will
163 enhance the positive effects of elevated CO₂ on total leaf area and total biomass. This
164 response will be due to increased belowground carbon allocation and nitrogen uptake and
165 with increasing nitrogen fertilization that will be stronger under elevated CO₂. Biomass
166 responses to elevated CO₂ will be driven by a greater increase in belowground biomass
167 than aboveground biomass, as plants will invest in resource acquisition strategies to meet
168 the increased whole-plant nitrogen demand for building new tissues.

169 (3) Following the nitrogen limitation hypothesis, inoculation with nitrogen-fixing bacteria
170 will enhance positive whole-plant responses to elevated CO₂. These responses will be
171 strongest under low nitrogen availability, where inoculated plants will invest in nitrogen
172 uptake through symbiotic nitrogen fixation over more costly direct uptake pathways.
173 However, these patterns will diminish with increasing nitrogen fertilization as plants
174 acquire more nitrogen through increasingly less costly direct uptake pathways.

175

176 **Materials and methods**

177 *Seed treatments and experimental design*

178 *Glycine max* L. (Merr) seeds (Territorial Seed Co., Cottage Grove, OR, USA) were planted in
179 144 6-liter surface sterilized pots (NS-600, Nursery Supplies, Orange, CA, USA) containing a
180 steam-sterilized 70:30 volume:volume mix of *Sphagnum* peat moss (Premier Horticulture,
181 Quakertown, PA, USA) to sand (Pavestone, Atlanta, GA, USA). Before planting, all *G. max*
182 seeds were surface sterilized in 2% sodium hypochlorite for 3 minutes, followed by three 3-
183 minute washes with ultrapure water (MilliQ 7000; MilliporeSigma, Burlington, MA USA).

184 Subsets of surface-sterilized seeds were inoculated with *Bradyrhizobium japonicum* (Verdesian

185 N-Dure™ Soybean, Cary, NC, USA) in a slurry following manufacturer recommendations (3.12
186 g inoculant and 241 g ultrapure water per 1 kg seed).

187 Seventy-two pots were randomly planted using surface-sterilized seeds inoculated with *B.*
188 *japonicum*, while the remaining 72 pots were planted using surface-sterilized uninoculated seeds.

189 Thirty-six pots in each inoculation treatment were placed in one of two atmospheric CO₂
190 treatments (420, 1000 µmol mol⁻¹ CO₂). CO₂ treatments were decided based on current ambient

191 CO₂ concentrations and projections from the Intergovernmental Panel on Climate Change

192 indicating that CO₂ concentrations could surpass 1000 ppm by 2100 under the Shared

193 Socioeconomic Pathway 5-8.5 (IPCC, 2021). Plants in each unique inoculation-by-CO₂

194 treatment combination received one of nine nitrogen fertilization treatments equivalent to 0 (0

195 mM), 35 (2.5 mM), 70 (5 mM), 105 (7.5 mM), 140 (10 mM), 210 (15 mM), 280 (20 mM), 350

196 (25 mM), or 630 ppm (45 mM) N. This experimental setup resulted in 4 replicates per unique

197 inoculation-by-CO₂-by-nitrogen fertilization treatment combination. Nitrogen fertilization

198 treatments were created using a modified Hoagland's solution (Hoagland and Arnon, 1950)

199 designed to keep concentrations of all other macronutrients and micronutrients equivalent across

200 treatments (Table S1). Plants received the same nitrogen fertilization treatment twice per week in

201 150 mL doses as topical agents to the soil surface. Plants were well-watered between fertilization

202 doses to ensure that physiology and growth was not limited by water availability.

203

204 *Growth chamber conditions*

205 Plants were randomly placed in one of six calibrated Percival LED-41L2 growth chambers

206 (Percival Scientific Inc., Perry, IA, USA) over two experimental iterations due to chamber space

207 limitation. The first iteration included all plants grown under elevated CO₂, while the second

208 included all plants grown under ambient CO₂. Average (\pm SD) CO₂ concentrations across
209 chambers throughout the experiment were 439 \pm 5 $\mu\text{mol mol}^{-1}$ CO₂ for the ambient treatment and
210 989 \pm 4 $\mu\text{mol mol}^{-1}$ CO₂ for the elevated treatment. Each experimental iteration lasted seven
211 weeks, which was sufficient for plants to grow through the majority of their vegetative growth
212 phase without evidence of reproduction.

213 Daytime growth conditions were simulated using a 16-hour photoperiod, with incoming
214 light radiation set to chamber maximum (mean \pm SD: 1230 \pm 12 $\mu\text{mol m}^{-2} \text{s}^{-1}$ across chambers), air
215 temperature set to 25°C, and relative humidity set to 50%. This daylength allowed plants to
216 maximize vegetative growth across the seven-week experiment while minimizing the onset of
217 reproduction. The remaining 8-hour period simulated nighttime growing conditions, with
218 incoming light radiation set to 0 $\mu\text{mol m}^{-2} \text{s}^{-1}$, chamber temperature set to 17°C, and relative
219 humidity set to 50%. Transitions between daytime and nighttime growing conditions were
220 simulated by ramping incoming light radiation in 45-minute increments and temperature in 90-
221 minute increments over 3 hours (Table S2).

222 Plants grew under average (\pm SD) daytime light intensity of 1049 \pm 27 $\mu\text{mol m}^{-2} \text{s}^{-1}$,
223 including ramping periods. In the elevated CO₂ iteration, plants grew under 24.0 \pm 0.2°C during
224 the day, 16.4 \pm 0.8°C during the night, and 51.6 \pm 0.4% relative humidity. In the ambient CO₂
225 iteration, plants grew under 23.9 \pm 0.2°C during the day, 16.0 \pm 1.4°C during the night, and
226 50.3 \pm 0.2% relative humidity. Any differences in climate conditions across the six chambers were
227 accounted for by shuffling the same group of plants throughout the growth chambers. This
228 process was done by iteratively moving the group of plants on the top rack of a chamber to the
229 bottom rack of the same chamber while simultaneously moving the group of plants on the

230 bottom rack of a chamber to the top rack of the adjacent chamber. Plants were moved within and
231 across chambers daily during each experiment iteration.

232

233 *Leaf gas exchange measurements*

234 Leaf gas exchange measurements were collected in all plants ($n = 144$ individuals) on the
235 seventh week of development, before the onset of reproduction. All gas exchange measurements
236 were collected on the center leaflet of the most recent fully expanded trifoliate leaflet set using
237 LI-6800 portable photosynthesis machines configured with a 6800-01A fluorometer head and 6
238 cm² aperture (LI-COR Biosciences, Lincoln, NE, USA). Specifically, net photosynthesis rates
239 (A_{net} ; $\mu\text{mol m}^{-2} \text{s}^{-1}$), stomatal conductance rates (g_{sw} ; $\text{mol m}^{-2} \text{s}^{-1}$), and intercellular CO₂
240 concentrations (C_i ; $\mu\text{mol mol}^{-1}$) were measured across a range of atmospheric CO₂
241 concentrations (i.e., an A_{net}/C_i curve) using the Dynamic Assimilation™ Technique. The
242 Dynamic Assimilation™ Technique corresponds well with traditional steady-state A_{net}/C_i curves
243 in *G. max* (Saathoff and Welles, 2021; Tejera-Nieves *et al.*, 2024). A_{net}/C_i curves were generated
244 along a reference CO₂ ramp down from 420 $\mu\text{mol mol}^{-1}$ CO₂ to 20 $\mu\text{mol mol}^{-1}$ CO₂, followed by
245 a ramp up from 420 $\mu\text{mol mol}^{-1}$ CO₂ to 1620 $\mu\text{mol mol}^{-1}$ CO₂ after a 90-second wait period at
246 420 $\mu\text{mol mol}^{-1}$ CO₂. The ramp rate for each curve was set to 200 $\mu\text{mol mol}^{-1} \text{min}^{-1}$, logging
247 every five seconds, generating 96 data points per response curve. All A_{net}/C_i curves were
248 conducted after A_{net} and g_{sw} stabilized in an LI-6800 cuvette set to a 500 mol s^{-1} flow rate, 10000
249 rpm mixing fan speed, 1.5 kPa vapor pressure deficit, 25°C leaf temperature, 2000 $\mu\text{mol m}^{-2} \text{s}^{-1}$
250 incoming light radiation, and initial reference CO₂ concentration set to 420 $\mu\text{mol mol}^{-1}$.

251 Snapshot A_{net} measurements were extracted from each A_{net}/C_i curve, both at a common
252 CO₂ concentration, 420 $\mu\text{mol mol}^{-1}$ CO₂ ($A_{\text{net},420}$; $\mu\text{mol m}^{-2} \text{s}^{-1}$), and growth CO₂ concentration,

253 420 and 1000 $\mu\text{mol mol}^{-1}$ CO_2 ($A_{\text{net,gc}}$; $\mu\text{mol m}^{-2} \text{s}^{-1}$). We quantified $A_{\text{net},420}$ to gauge relative
254 investment in photosynthetic tissues between treatment combinations and $A_{\text{net,gc}}$ to quantify
255 photosynthetic performance between treatment combinations. Dark respiration (R_d ; $\mu\text{mol m}^{-2} \text{s}^{-1}$)
256 measurements were collected on the same leaflet used to generate A_{net}/C_i curves following at
257 least a 30-minute period of darkness. Dark respiration measurements were collected on a 5-
258 second log interval for 60 seconds after the leaf stabilized in an LI-6800 cuvette set to a 500 mol
259 s^{-1} flow rate, 10000 rpm mixing fan speed, 1.5 kPa vapor pressure deficit, 25°C leaf temperature,
260 and 420 $\mu\text{mol mol}^{-1}$ reference CO_2 concentration (regardless of CO_2 treatment), with incoming
261 light radiation set to 0 $\mu\text{mol m}^{-2} \text{s}^{-1}$. A single dark respiration value was determined for each
262 leaflet by calculating the mean dark respiration value across the logging interval.

263

264 *A/C_i curve-fitting and parameter estimation*

265 A_{net}/C_i curves were fit using the ‘fitaci’ function in the ‘plantecophys’ R package (Duursma,
266 2015). This function estimates the apparent maximum rate of Rubisco carboxylation (V_{cmax} ;
267 $\mu\text{mol m}^{-2} \text{s}^{-1}$) and apparent maximum rate of electron transport for RuBP regeneration (J_{max} ;
268 $\mu\text{mol m}^{-2} \text{s}^{-1}$) based on the Farquhar et al. (1980) biochemical model of C₃ photosynthesis. Triose
269 phosphate utilization (TPU) limitation was included as an additional rate-limiting step after
270 visually observing clear TPU limitation for most curves. All curve fits included measured dark
271 respiration values. As A_{net}/C_i curves were generated using a common leaf temperature (25°C),
272 curves were fit using Michaelis-Menten coefficients for Rubisco affinity to CO_2 (K_c ; $\mu\text{mol mol}^{-1}$)
273 and O_2 (K_o ; mmol mol^{-1}), and the CO_2 compensation point (I^* ; $\mu\text{mol mol}^{-1}$) reported in
274 Bernacchi et al. (2001). Specifically, K_c was set to 404.9 $\mu\text{mol mol}^{-1}$, K_o was set to 278.4 μmol

275 mol⁻¹, and I^* was set to 42.75 $\mu\text{mol mol}^{-1}$. V_{cmax} , J_{max} , and R_{d} estimates are referenced throughout
276 the rest of the paper as V_{cmax25} , J_{max25} , and R_{d25} .

277

278 *Leaf trait measurements*

279 The leaflet used for A_{net}/C_i curves and dark respiration measurements was harvested immediately
280 following gas exchange measurements. Images of each focal leaflet were curated using a flat-bed
281 scanner to determine fresh leaf area using the 'LeafArea' R package (Katabuchi, 2015), which
282 automates leaf area calculations using ImageJ software (Schneider *et al.*, 2012). Post-processed
283 images were visually assessed to check against errors in the automation process. Each focal
284 leaflet was dried at 65°C for at least 48 hours, weighed, and ground until homogenized. Leaf
285 mass per area (M_{area} ; g m⁻²) was calculated as the ratio of dry leaflet biomass to fresh leaflet area.
286 Leaf nitrogen content (N_{mass} ; gN g⁻¹) was quantified using a subsample of ground and
287 homogenized leaflet tissue through elemental combustion (Costech-4010, Costech, Inc.,
288 Valencia, CA, USA). Leaf nitrogen content per unit leaf area (N_{area} ; gN m⁻²) was calculated by
289 multiplying N_{mass} and M_{area} . Photosynthetic nitrogen-use efficiency ($PNUE_{\text{gc}}$; $\mu\text{mol CO}_2 \text{ g}^{-1} \text{ N s}^{-1}$)
290 was estimated as the ratio of $A_{\text{net,gc}}$ to N_{area} .

291 Chlorophyll content was extracted from a second leaflet in the same trifoliate leaf set as
292 the leaf used to generate A_{net}/C_i curves. A cork borer was used to punch 3-5 0.6 cm² disks from
293 the leaflet. Images of each set of leaflet disks were curated using a flat-bed scanner to determine
294 wet leaf area using the 'LeafArea' R package (Katabuchi, 2015). Leaflet disks were shuttled into
295 a test tube containing 10 mL dimethyl sulfoxide, vortexed, and incubated at 65°C for 120
296 minutes (Barnes *et al.*, 1992). Incubated test tubes were vortexed again before being loaded in
297 150 μL triplicate aliquots to a 96-well plate. Dimethyl sulfoxide was loaded in each plate as a

298 single 150 μL triplicate aliquot and used as a blank. Absorbance measurements at 649 nm (A_{649})
299 and 665 nm (A_{665}) were recorded using a plate reader (Biotek Synergy H1; Biotek Instruments,
300 Winooski, VT USA), with triplicate measurements averaged and corrected by the mean of the
301 blank absorbance value. Blank-corrected absorbance values were used to estimate chlorophyll *a*
302 (Chl_a ; $\mu\text{g mL}^{-1}$) and chlorophyll *b* (Chl_b ; $\mu\text{g mL}^{-1}$) following equations from Wellburn (1994):

303 $Chl_a = 12.19A_{665} - 3.45A_{649}$ (1)

304 and

305 $Chl_b = 21.99A_{649} - 5.32A_{665}$ (2)

306 Chl_a and Chl_b were converted to mmol mL^{-1} using the molar masses of chlorophyll *a* (893.51 g
307 mol^{-1}) and chlorophyll *b* (907.47 g mol^{-1}), then added together to calculate the total chlorophyll
308 content in dimethyl sulfoxide extractant (mmol mL^{-1}). Total chlorophyll content (mmol) was
309 determined by multiplying the total chlorophyll content in dimethyl sulfoxide by the volume of
310 dimethyl sulfoxide extractant (10 mL). Area-based chlorophyll content (Chl_{area} ; mmol m^{-2}) was
311 calculated by dividing the total chlorophyll content by the total area of the leaflet disks.

312

313 *Whole-plant measurements*

314 All individuals were harvested, and biomass of major organ types (leaves, stems, roots, and
315 nodules when present) were separated immediately following gas exchange measurements on the
316 seventh week of development. Fresh leaf area of all harvested leaflets was measured using an LI-
317 3100C (LI-COR Biosciences, Lincoln, Nebraska, USA). Total fresh leaf area (cm^2) was
318 calculated as the sum of all leaflet areas, including those used for gas exchange and chlorophyll
319 extractions. Harvested material was separately dried in an oven set to 65°C for at least 48 hours
320 to a constant mass, weighed, and then ground to homogeneity. Leaves and root nodules were

321 ground using a mortar and pestle, while stems and roots were ground using an E3300 Single
322 Speed Mini Cutting Mill (Eberbach Corp., MI, USA). Total biomass (g) was calculated as the
323 sum of dry leaf, stem, root, and root nodule biomass. Carbon and nitrogen content was measured
324 for each organ type through elemental combustion (Costech-4010, Costech, Inc., Valencia, CA,
325 USA) using ground and homogenized organ tissue subsamples. The ratio of root nodule biomass
326 to root biomass was calculated as an indicator of plant investment toward nitrogen fixation
327 relative to other uptake pathways (e.g., direct uptake). The root:shoot ratio (unitless) was
328 calculated as the ratio of belowground biomass (root and root nodule biomass) to shoot biomass
329 (leaf and stem biomass). Leaf, stem, and root mass fractions were calculated as the dry biomass
330 of each respective organ per unit total biomass (g g^{-1} in all cases).

331 Belowground biomass carbon costs to acquire nitrogen were quantified as the ratio of
332 belowground biomass carbon to whole-plant nitrogen biomass (g C g N^{-1}) (Perkowski *et al.*,
333 2021). Belowground biomass carbon (g C) was calculated as the sum of root and root nodule
334 carbon biomass. Root carbon biomass and root nodule carbon biomass were calculated as the
335 product of the organ biomass and respective organ carbon content. Whole-plant nitrogen biomass
336 (g N) was calculated as the sum of total leaf, stem, root, and root nodule nitrogen biomass. Leaf,
337 stem, root, and root nodule nitrogen biomass was calculated as the product of the organ biomass
338 and respective organ nitrogen content. This calculation does not account for additional carbon
339 costs associated with respiration, root exudation, or root turnover and may underestimate carbon
340 costs to acquire nitrogen (Perkowski *et al.*, 2021).

341

342 *Statistical analyses*

343 Uninoculated plants with substantial root nodule formation (root nodule biomass: root biomass
344 values greater than 0.05 g g^{-1}) were removed from analyses following the assumption that plants
345 were incompletely sterilized or contaminated. This decision resulted in the removal of sixteen
346 plants from the analysis: two plants in the elevated CO₂ treatment that received 35 ppm N, three
347 plants in the elevated CO₂ treatment that received 70 ppm N, one plant in the elevated CO₂
348 treatment that received 210 ppm N, two plants in the elevated CO₂ treatment that received 280
349 ppm N, two plants in the ambient CO₂ treatment that received 0 ppm N, three plants in the
350 ambient CO₂ treatment that received 70 ppm N, two plants in the ambient CO₂ treatment that
351 received 105 ppm N, and one plant in the ambient CO₂ treatment that received 280 ppm N. A
352 summary of the replication scheme after these individuals were removed is included in the
353 *Supplemental Information* (Table S3-4).

354 A series of linear mixed-effects models were built to investigate the impacts of CO₂
355 concentration, nitrogen fertilization, and inoculation on *G. max* leaf nitrogen content, leaf gas
356 exchange, total leaf area, biomass, biomass allocation, and plant investment in symbiotic
357 nitrogen fixation. All models included CO₂ treatment as a categorical fixed effect, inoculation
358 treatment as a categorical fixed effect, and nitrogen fertilization as a continuous fixed effect, with
359 all possible interaction terms between all three fixed effects included. Models accounted for
360 climatic differences between chambers across experiment iterations by including a random
361 intercept term that nested the starting chamber rack within CO₂ treatment. Models with this
362 independent variable structure were created for each of the following dependent variables: N_{area} ,
363 M_{area} , N_{mass} , Chl_{area} , $A_{\text{net},420}$, $A_{\text{net,gc}}$, V_{cmax25} , J_{max25} , $J_{\text{max25}}:V_{\text{cmax25}}$, R_{d25} , $PNUE_{\text{gc}}$, total leaf area,
364 total biomass, total leaf biomass, stem biomass, root biomass, root nodule biomass, root:shoot
365 ratio, leaf mass fraction, stem mass fraction, root mass fraction, belowground biomass carbon

366 costs to acquire nitrogen, belowground biomass carbon, whole-plant nitrogen biomass, and the
367 root nodule biomass:root biomass ratio.

368 Shapiro-Wilk tests of normality were used to assess whether linear mixed-effects models
369 satisfied residual normality assumptions. Models for N_{area} , N_{mass} , Chl_{area} , $A_{\text{net},420}$, $A_{\text{net,gc}}$, $V_{\text{cmax}25}$,
370 $J_{\text{max}25}$, $J_{\text{max}25}:V_{\text{cmax}25}$, $R_{\text{d}25}$, $PNUE_{\text{gc}}$, total leaf area, leaf mass fraction, stem mass fraction,
371 belowground biomass carbon, and whole-plant nitrogen biomass satisfied residual normality
372 assumptions without data transformation. Models for M_{area} , root:shoot ratio, belowground
373 biomass carbon costs to acquire nitrogen, and root mass fraction satisfied residual normality
374 assumptions with a natural log data transformation. Models for total biomass, leaf biomass, stem
375 biomass, root biomass, root nodule biomass, and root nodule biomass: root biomass satisfied
376 residual normality assumptions with a square root data transformation.

377 In all models, the ‘lmer’ function in the ‘lme4’ R package (Bates *et al.*, 2015) was used to
378 fit each model, and the ‘Anova’ function in the ‘car’ R package (Fox and Weisberg, 2019) was
379 used to calculate Type II Wald's χ^2 and determine the significance ($\alpha=0.05$) of each fixed effect
380 coefficient. The ‘emmeans’ R package (Lenth, 2019) was used to conduct post-hoc comparisons
381 using Tukey's tests, where degrees of freedom were approximated using the Kenward-Roger
382 approach (Kenward and Roger, 1997). Trendlines and error ribbons representing the 95%
383 confidence intervals were drawn in all figures using ‘emmeans’ outputs across the range in
384 nitrogen fertilization values with a maximum of 36 data points per trendline (Table S4). All
385 analyses and plots were conducted in R version 4.1.0 (R Core Team, 2021). Results for N_{mass} and
386 M_{area} and organ biomasses are summarized in the *Supplemental Material* (Table S5, S7; Fig. S1).

387

388

389 **Results**

390 *Leaf nitrogen content*

391 Elevated CO₂ reduced N_{area} and Chl_{area} by 29% and 30%, respectively ($p<0.001$ in both cases; Table 1; Fig. 1). Increasing nitrogen fertilization increased N_{area} ($p<0.001$; Table 1; Fig. 1) more strongly under ambient CO₂ than elevated CO₂ (CO₂-by-nitrogen fertilization interaction: $p<0.05$; Table 1), resulting in a stronger reduction in N_{area} under elevated CO₂ as nitrogen fertilization increased (Fig. S2). Uninoculated plants experienced a stronger reduction in N_{area} under elevated CO₂ than inoculated plants (CO₂-by-inoculation interaction: $p<0.05$; Table 1). Increasing nitrogen fertilization increased N_{area} and Chl_{area} ($p<0.001$ in both cases; Table 1; Fig. 1) more strongly in uninoculated plants than inoculated plants (inoculation-by-nitrogen fertilization interaction: $p<0.001$ in both cases; Table 1).

400

401 *Gas exchange*

402 Elevated CO₂ decreased $A_{\text{net},420}$ by 17% and increased $A_{\text{net},\text{gc}}$ by 33% ($p<0.001$ in both cases; Table 2). Increasing nitrogen fertilization increased $A_{\text{net},420}$ and $A_{\text{net},\text{gc}}$ similarly between CO₂ treatments (CO₂-by-nitrogen fertilization interaction: $p>0.05$; Table 2; Fig. 2a). Inoculated plants experienced a stronger increase in $A_{\text{net},\text{gc}}$ under elevated CO₂ than uninoculated plants (CO₂-by-inoculation interaction: $p<0.05$; Table 2). Increasing nitrogen fertilization increased $A_{\text{net},420}$ and $A_{\text{net},\text{gc}}$ ($p<0.001$ in both cases; Table 2) more strongly in uninoculated plants than inoculated plants (inoculation-by-nitrogen fertilization interaction: $p<0.001$ in both cases; Fig. 2a-b).

409 Elevated CO₂ decreased $V_{\text{cmax}25}$ by 16% and $J_{\text{max}25}$ by 10%, increasing $J_{\text{max}25}:V_{\text{cmax}25}$ by 8% ($p<0.05$ in all cases; Table 2). Increasing nitrogen fertilization increased $V_{\text{cmax}25}$ and $J_{\text{max}25}$, but decreased $J_{\text{max}25}:V_{\text{cmax}25}$, similarly between CO₂ (CO₂-by-nitrogen fertilization interaction:

412 $p>0.05$ in all cases; Table 2; Fig. 2b-d) and inoculation treatments (CO_2 -by-inoculation
413 interaction: $p>0.05$ in all cases; Table 2). Increasing nitrogen fertilization increased $V_{\text{cmax}25}$ and
414 $J_{\text{max}25}$ and decreased $J_{\text{max}25}:V_{\text{cmax}25}$ ($p<0.001$; Table 2), but these patterns were only observed in
415 uninoculated plants (inoculation-by-nitrogen fertilization interaction: $p<0.05$ in all cases).

416 CO_2 treatment did not affect $R_{\text{d}25}$ ($p>0.05$; Table S6). Increasing nitrogen fertilization
417 increased $R_{\text{d}25}$ ($p<0.05$; Table S6), but this pattern was only observed in uninoculated plants
418 (inoculation-by-nitrogen fertilization interaction: $p<0.001$; Table S6; Fig. S3a). Inoculated plants
419 exhibited marginally greater $R_{\text{d}25}$ than uninoculated plants ($p<0.1$; Table S6)

420

421 *Photosynthetic nitrogen-use efficiency*

422 Elevated CO_2 increased PNUE_{gc} by 97% ($p<0.001$; Table S6; Fig. S3b) due to a 33% increase in
423 $A_{\text{net},\text{gc}}$ (Fig. 2a) and 29% decrease in N_{area} (Fig. 1a). Increasing nitrogen fertilization decreased
424 PNUE_{gc} ($p<0.001$; Table S6) more strongly under elevated CO_2 (CO_2 -by-nitrogen fertilization
425 interaction: $p<0.05$; Table S6; Fig. S3b), leading to a weaker increase in PNUE_{gc} due to elevated
426 CO_2 as nitrogen fertilization increased (Fig. S6). Increasing nitrogen fertilization decreased
427 PNUE_{gc} ($p<0.001$; Table S6), but this pattern was only observed in inoculated plants
428 (inoculation-by-nitrogen fertilization interaction: $p<0.05$; Table S6; Fig. S3b).

429

430 *Total leaf area and total biomass*

431 Elevated CO_2 increased total leaf area and total biomass by 51% and 102%, respectively
432 ($p<0.001$ in both cases; Table 3). Increasing nitrogen fertilization increased total leaf area and
433 total biomass ($p<0.001$ in both cases; Table 3) more strongly under elevated CO_2 than ambient
434 CO_2 (CO_2 -by-nitrogen fertilization interaction: $p<0.001$ in both cases; Table 3), leading to an

435 amplified positive effect of elevated CO₂ on total leaf area and total biomass as nitrogen
436 fertilization increased (Fig. 3a-b). Inoculation had no effect on total leaf area or total biomass
437 responses to elevated CO₂ (CO₂-by-inoculation interaction: $p>0.05$ in both cases; Table 3).
438 Increasing nitrogen fertilization increased total leaf area and total biomass ($p<0.001$ in both
439 cases; Table 3) more strongly in uninoculated plants than inoculated plants (inoculation-by-
440 nitrogen fertilization interaction: $p<0.001$; Table 3; Fig. 3a-b).

441

442 *Biomass partitioning*

443 The root:shoot ratio decreased under elevated CO₂ ($p<0.05$; Table 3; Fig. 3c), although this
444 pattern was only observed in inoculated plants (CO₂-by-inoculation interaction: $p<0.05$; Table 3,
445 Fig. 3c). Reductions in the root:shoot ratio under elevated CO₂ were driven by an increase in the
446 leaf mass fraction under elevated CO₂ ($p<0.001$; Table S7) that was only observed in inoculated
447 plants (CO₂-by-inoculation interaction: $p<0.05$; Table S7). CO₂ treatment did not affect stem
448 mass fraction ($p>0.05$; Table S7), although an interaction between CO₂ and inoculation treatment
449 indicated that elevated CO₂ increased the root mass fraction in inoculated plants (CO₂-by-
450 inoculation interaction: $p<0.05$; Table S7). Increasing nitrogen fertilization decreased the
451 root:shoot ratio ($p<0.001$; Table 3), a pattern that was marginally stronger in uninoculated plants
452 than inoculated plants (CO₂-by-inoculation interaction: $p=0.051$; Table 3; Fig. 3c). Increasing
453 nitrogen fertilization increased the leaf mass fraction and decreased the root mass fraction
454 ($p<0.001$ in both cases; Table S7), but these patterns only occurred in uninoculated plants
455 (inoculation-by-nitrogen fertilization interaction: $p<0.05$ in both cases; Table S7). Increasing
456 nitrogen fertilization increased stem mass fraction ($p<0.001$; Table S7), but these patterns only

457 occurred in inoculated plants (inoculation-by-nitrogen fertilization interaction: $p<0.001$; Table
458 S7).

459

460 *Belowground biomass carbon cost to acquire nitrogen*

461 Elevated CO₂ increased belowground biomass carbon costs to acquire nitrogen ($p<0.001$; Table
462 3) more strongly in uninoculated plants than inoculated plants (CO₂-by-inoculation interaction:
463 $p<0.001$; Table 3). Increasing nitrogen fertilization decreased carbon costs to acquire nitrogen
464 ($p<0.001$; Table 3) more strongly in uninoculated plants than inoculated plants (inoculation-by-
465 nitrogen fertilization: $p<0.001$; Table 3; Fig. 3d). Interactions between inoculation and nitrogen
466 fertilization treatments were more pronounced when plants were grown under elevated CO₂
467 (CO₂-by-inoculation-by-nitrogen fertilization interaction: $p<0.05$; Fig. 3d). This pattern was
468 driven by a strong negative effect of increasing nitrogen fertilization on carbon costs to acquire
469 nitrogen in uninoculated plants grown under elevated CO₂ (Tukey: $p<0.001$) coupled with no
470 nitrogen fertilization effect in inoculated plants grown under elevated CO₂ (Tukey: $p<0.001$).
471 Under ambient CO₂, increasing nitrogen fertilization decreased carbon costs to acquire nitrogen
472 similarly between inoculation treatments (Tukey: $p>0.05$).

473 Elevated CO₂ increased belowground biomass carbon by 93% and increased whole-plant
474 nitrogen biomass by 26% ($p<0.001$ in both cases; Table S8). Increasing nitrogen fertilization
475 increased belowground biomass carbon and whole-plant nitrogen biomass more strongly under
476 elevated CO₂ than ambient CO₂ (CO₂-by-nitrogen fertilization interaction: $p<0.001$; Table S8;
477 Fig. S5). These patterns resulted in an amplified positive effect of elevated CO₂ on belowground
478 biomass carbon and whole-plant nitrogen biomass as nitrogen fertilization increased, though this
479 pattern was stronger for whole-plant nitrogen biomass than belowground biomass carbon (Fig.

480 S5). Increasing nitrogen fertilization increased belowground biomass carbon and whole-plant
481 nitrogen biomass ($p<0.001$; Table S8) more strongly in uninoculated plants than inoculated
482 plants (inoculation-by-nitrogen fertilization interaction: $p<0.001$ in both cases; Table S8; Fig.
483 S5).

484

485 *Plant investment toward symbiotic nitrogen fixation*

486 CO₂ treatment did not affect root nodule: root biomass ($p>0.05$; Table 3; Fig. 4) despite
487 anecdotally stronger positive effects of elevated CO₂ on root biomass (96% increase; $p<0.001$;
488 Table S7) than root nodule biomass (70% increase; $p<0.001$; Table S7). Increasing nitrogen
489 fertilization decreased root nodule: root biomass ($p<0.001$; Table 3) more strongly in inoculated
490 plants than uninoculated plants (inoculation-by-nitrogen fertilization interaction: $p<0.001$; Table
491 3; Fig. 4).

492

493 **Discussion**

494 *Glycine max* plants were grown under two CO₂ concentrations, two inoculation treatments, and
495 nine nitrogen fertilization treatments in a full-factorial growth chamber experiment. We used
496 data collected from this experiment to (1) determine whether plant responses to elevated CO₂
497 aligned more closely with the nitrogen limitation or eco-evolutionary optimality hypothesis and
498 (2) assess how the ability to associate with symbiotic nitrogen-fixing bacteria might influence
499 these responses.

500

501 *Leaf photosynthetic responses to elevated CO₂ are unrelated to nitrogen availability*

502 Individuals grown under elevated CO₂ experienced a reduction in $A_{\text{net},420}$ (Table 2), leaf nitrogen
503 content (Fig. 1a, S1), $V_{\text{cmax}25}$ (Fig. 2b), and $J_{\text{max}25}$ (Fig. 2c) compared to plants grown under
504 ambient CO₂. These patterns suggest a downregulation of leaf-level investment toward
505 photosynthetic enzymes under elevated CO₂. This downregulation was likely driven by increased
506 Rubisco affinity for carboxylation relative to oxygenation, which decreased leaf-level demand to
507 build and maintain photosynthetic enzymes (Bazzaz, 1990; Dong *et al.*, 2022). Despite reduced
508 investment toward photosynthetic enzymes, elevated CO₂ increased $A_{\text{net},\text{gc}}$ (Fig. 2a). This
509 response was associated with a reduction in N_{area} and a larger reduction in $V_{\text{cmax}25}$ than $J_{\text{max}25}$,
510 which increased photosynthetic nitrogen-use efficiency (Fig. S3b) and $J_{\text{max}25}:V_{\text{cmax}25}$ and allowed
511 enhanced $A_{\text{net},\text{gc}}$ to be achieved by approaching optimal coordination (Chen *et al.*, 1993; Maire *et*
512 *al.*, 2012; Smith and Keenan, 2020). These patterns are consistent with our expectations and
513 previous studies that have investigated leaf photosynthetic responses to elevated CO₂ (Drake *et*
514 *al.*, 1997; Ainsworth *et al.*, 2002; Ainsworth and Long, 2005; Ainsworth and Rogers, 2007;
515 Crous *et al.*, 2010; Lee *et al.*, 2011; Smith and Dukes, 2013; Poorter *et al.*, 2022; Cui *et al.*,
516 2023; Stocker *et al.*, 2025).

517 Positive effects of elevated CO₂ on $A_{\text{net},\text{gc}}$ (Fig. 2a) and $J_{\text{max}25}:V_{\text{cmax}25}$ (Fig. 2d) and
518 negative effects of elevated CO₂ on $A_{\text{net},420}$, $V_{\text{cmax}25}$, and $J_{\text{max}25}$ (Figs. 2a-c) were not modified by
519 nitrogen fertilization, as the slope that explained the effects of increasing nitrogen fertilization on
520 each of these traits was similar between CO₂ treatments. Instead, the increase in $J_{\text{max}25}:V_{\text{cmax}25}$
521 (Fig. 2d) and PNUE_{gc} (Fig. S3b) under elevated CO₂ provides strong support for the idea that
522 leaves were downregulating $V_{\text{cmax}25}$ in response to elevated CO₂ such that enhanced $A_{\text{net},\text{gc}}$ could
523 be achieved by approaching optimal coordination of Rubisco carboxylation and electron
524 transport for RuBP regeneration (Chen *et al.*, 1993; Maire *et al.*, 2012; Smith and Keenan, 2020).

525 Negative effects of elevated CO₂ on mass- and area-based leaf nitrogen content became
526 more pronounced with increasing nitrogen fertilization (Fig. S2a-b). Since nitrogen fertilization
527 did not affect photosynthetic responses to elevated CO₂, this decline in leaf nitrogen content may
528 reflect reduced allocation to non-photosynthetic pools, such as structural tissue or chemical
529 pathways that contribute to herbivore defense (Zavala *et al.*, 2013; Onoda *et al.*, 2017; Johnson
530 *et al.*, 2020). While not a primary focus of this study, understanding leaf nitrogen allocation
531 responses to elevated CO₂ across nitrogen availability gradients would help clarify the role of
532 leaf nitrogen allocation on leaf-level responses to elevated CO₂.

533 Overall, leaf photosynthetic responses to elevated CO₂ showed strong support for the
534 eco-evolutionary optimality hypothesis. Photosynthetic responses to elevated CO₂ were
535 independent from nitrogen fertilization, suggesting that these responses were wholly determined
536 through changes in leaf-level demand to build and maintain photosynthetic enzymes. These
537 findings also reinforce previous work showing that leaf photosynthetic responses to elevated CO₂
538 are decoupled from nitrogen availability (Lee *et al.*, 2011; Pastore *et al.*, 2019; Smith and
539 Keenan, 2020; Harrison *et al.*, 2021). Additionally, our results indicate that optimal resource
540 investment to photosynthetic capacity may function as a nitrogen-savings mechanism that allows
541 plants to maximize resource-use efficiency at the leaf-level as a strategy for maximizing resource
542 allocation to whole-plant growth (Smith and Keenan, 2020; Smith *et al.*, 2024).

543
544 *Whole-plant responses to elevated CO₂ are constrained by nitrogen availability*
545 Leaf photosynthetic responses to elevated CO₂ corresponded with increased total leaf area and
546 total biomass (Fig. 3a-b), supporting previous work (Ainsworth *et al.*, 2002; Ainsworth and
547 Long, 2005; Smith and Dukes, 2013; Poorter *et al.*, 2022; Stocker *et al.*, 2025). Increased total

548 leaf area increased whole-plant capacity for light interception, boosting whole-plant
549 photosynthesis and supporting biomass accumulation when coupled with an increase in leaf-level
550 $A_{\text{net,gc}}$. Contrasting expectations and previous work (Nie *et al.*, 2013; Stocker *et al.*, 2025),
551 elevated CO₂ decreased the root-to-shoot ratio (Fig. 3c) through an increase in the leaf mass
552 fraction and no change in the stem or root mass fractions (Table S7). Despite this, plants
553 experienced an increase in root biomass (Fig. S6b) and belowground carbon allocation (Fig. S5a)
554 under elevated CO₂, suggesting that plants responded to heightened whole-plant demand under
555 elevated CO₂ by investing in structures that support nutrient acquisition even if they allocated
556 relatively more biomass aboveground .

557 Increasing nitrogen fertilization enhanced the positive effects of elevated CO₂ on total
558 leaf area and total biomass (Fig. 3a-b). Interestingly, this interaction revealed no effect of CO₂
559 treatment on total leaf area in uninoculated individuals under low nitrogen fertilization,
560 supporting previous work showing that CO₂ fertilization effects on traits related to whole-plant
561 growth are often absent under low nutrient availability (Sigurdsson *et al.*, 2013). Similar effects
562 of CO₂ treatment on total leaf area under low nitrogen fertilization may have been due to plants
563 being unable to satisfy demand for soil nitrogen similarly between the two CO₂ treatments.
564 Stronger positive effects of elevated CO₂ on total leaf area and total biomass with increasing
565 nitrogen fertilization were associated with stronger increases in belowground carbon allocation
566 and whole-plant nitrogen uptake (Fig. S5), supporting the nitrogen limitation hypothesis (Luo *et*
567 *al.*, 2004; Reich *et al.*, 2006; Norby *et al.*, 2010; Feng *et al.*, 2015). These findings indicate that
568 plants grown under elevated CO₂ satisfied the greater whole-plant demand to build new tissues
569 by increasing investment to nitrogen acquisition, suggesting that whole-plant responses to
570 elevated CO₂ were constrained by nitrogen availability as expected. Despite this, nitrogen

571 availability did not modify whether plants invested in aboveground or belowground tissues, as
572 indicated by similar positive effects of increasing nitrogen fertilization on the root-to-shoot ratio
573 (Fig. 3c) and all organ mass fractions between CO₂ treatments (Table S7). These responses
574 indicate that biomass allocation responses to elevated CO₂ were more strongly dictated by
575 changes in whole-plant demand to build new tissues than the supply of nutrients.

576

577 *Inoculation does not affect leaf or whole-plant responses to elevated CO₂*
578 Inoculation increased N_{area} (Fig. 1a), $A_{\text{net},420}$, $A_{\text{net},\text{gc}}$ (Fig. 2a), $V_{\text{cmax}25}$ (Fig. 2b), $J_{\text{max}25}$ (Fig. 2c),
579 total leaf area (Fig. 3a), and total biomass (Fig. 3b), but decreased $J_{\text{max}25}:V_{\text{cmax}25}$ (Fig. 2d). These
580 results support previous studies suggesting that species forming symbiotic associations with
581 nitrogen-fixing bacteria have greater leaf nitrogen content, photosynthetic capacity, and growth
582 than those that do not (Adams *et al.*, 2016; Bytnarowicz *et al.*, 2023). The positive effects of
583 inoculation on leaf and whole-plant traits were strongest under low nitrogen fertilization and
584 diminished with increasing nitrogen fertilization, likely due to a reduction in plant investment
585 toward symbiotic nitrogen fixation (Fig. 4). These patterns support the idea that forming
586 associations with symbiotic nitrogen-fixing bacteria confers a competitive advantage in nitrogen-
587 limited environments, where access to a less-finite nitrogen pool (i.e., the atmosphere) allows
588 plants to satisfy leaf- and whole-plant demand more efficiently than relying on limited soil
589 nitrogen (Rastetter *et al.*, 2001; Andrews *et al.*, 2011; McCulloch and Porder, 2021).

590 Inoculation largely had no effect on leaf- or whole-plant responses to elevated CO₂, but
591 played a strong role in determining the effect of nitrogen fertilization on measured traits. This
592 null inoculation effect on plant responses to elevated CO₂ was consistent across the nitrogen
593 fertilization gradient, which contrasts our hypothesis that inoculation would enhance plant

594 responses to elevated CO₂ most strongly under low nitrogen fertilization (Rastetter *et al.*, 2001;
595 Perkowski *et al.*, 2021). Previous research has highlighted that nitrogen-fixing species typically
596 show stronger responses to elevated CO₂ than non-fixing species (Ainsworth *et al.*, 2002;
597 Ainsworth and Long, 2005), although some studies question the generality of this pattern
598 (Nowak *et al.*, 2004; Rogers *et al.*, 2009). Our findings assert that the ability to associate with
599 symbiotic nitrogen-fixing bacteria played no role in determining whether plant responses to
600 elevated CO₂ aligned with the nitrogen limitation or eco-evolutionary optimality hypotheses,
601 even though inoculated individuals grown under elevated CO₂ exhibited greater root nodule
602 biomass (Fig. S6a) and reduced carbon costs to acquire nitrogen (Fig. 3d) compared to those
603 grown under ambient CO₂.

604 As mentioned above, plants grown under elevated CO₂ exhibited an increase in root
605 nodule biomass (Fig. S6a). This pattern indicates that plants responded to heightened whole-
606 plant demand for new tissue growth by increasing nitrogen uptake through nitrogen fixation.
607 However, the increase in root nodule biomass was circumvented by a stronger increase in root
608 biomass (Fig. S6b). This pattern indicates an investment shift toward direct uptake with
609 increasing CO₂, a response that runs counter to previous work showing that plants increase
610 investment in microbial symbionts when whole-plant demand to build new tissues increases
611 (Taylor and Menge, 2018; Friel and Friesen, 2019; Perkowski *et al.*, 2021). If true, increased
612 relative allocation to root biomass may have been a strategy to prioritize the acquisition of non-
613 nitrogen resources, as nitrogen fixation may increase the extent by which physiology and plant
614 growth becomes limited by other nutrients, such as phosphorus (Finzi and Rodgers, 2009).
615 Previous research has shown that phosphorus plays a key role in shaping plant responses to
616 elevated CO₂ and that the benefits of nitrogen fixation under elevated CO₂ become more

617 apparent when other nutrients, such as phosphorus, are also available in sufficient supply (van
618 Groenigen *et al.*, 2006; Jiang *et al.*, 2020). Thus, it is possible that the null effects of inoculation
619 on plant responses to elevated CO₂ may have been driven by phosphorus colimitation, although
620 future work is needed to test this hypothesis.

621

622 *Modeling implications*

623 Many terrestrial biosphere models predict photosynthetic capacity through parameterized
624 relationships between N_{area} and V_{cmax} (Smith and Dukes, 2013; Rogers *et al.*, 2017), which
625 assumes that leaf nitrogen-photosynthesis relationships are constant across growing
626 environments. Our results build on previous work suggesting that leaf nitrogen-photosynthesis
627 relationships dynamically change across growing environments (Luo *et al.*, 2021; Waring *et al.*,
628 2023). Specifically, elevated CO₂ reduced leaf nitrogen content (Fig. 1a) more strongly than it
629 increased $A_{\text{net,gc}}$ (Fig. 2a) and decreased $V_{\text{cmax}25}$ (Fig. 2b) and $J_{\text{max}25}$ (Fig. 2c), while inoculation
630 increased $V_{\text{cmax}25}$ and $J_{\text{max}25}$ more strongly than it increased leaf nitrogen content. These patterns
631 indicate that elevated CO₂ increased the fractional pool of leaf nitrogen content allocated to
632 Rubisco and bioenergetics, while inoculation decreased the fraction of leaf nitrogen content
633 allocated to Rubisco and bioenergetics (Niinemets and Tenhunen, 1997).

634 Increasing nitrogen fertilization increased indices of apparent photosynthetic capacity,
635 but this pattern was only observed in uninoculated plants. Increasing nitrogen fertilization also
636 increased N_{area} and Chl_{area} more strongly in uninoculated plants (Fig. 1). Eco-evolutionary
637 optimality theory predicts that plants should exhibit strong positive effects of increasing nitrogen
638 availability on photosynthetic traits when nitrogen availability is insufficient for satisfying leaf-
639 level demand for building and maintaining photosynthetic enzymes, or when changes in nitrogen

640 availability decrease the relative costs of nitrogen acquisition and use compared to those of water
641 acquisition and use (Wright *et al.*, 2003; Harrison *et al.*, 2021; Stocker *et al.*, 2025). In such
642 cases where nitrogen availability exceeds leaf-level demand for photosynthetic enzymes or costs
643 to acquire nitrogen relative to water increase, the theory predicts that positive effects of
644 increasing nitrogen availability on photosynthesis should diminish, with excess nitrogen not
645 needed to satisfy leaf-level demand for photosynthesis being allocated toward the construction of
646 other plant tissues (e.g., additional leaves). Given this, strong positive effects of increasing
647 nitrogen fertilization on indices of photosynthetic capacity in uninoculated plants were expected,
648 as uninoculated plants were nitrogen-limited under low nitrogen fertilization and could not meet
649 the leaf-level demand for photosynthetic enzymes. We also found some evidence for a
650 diminished positive effect of nitrogen fertilization on photosynthetic traits, with uninoculated
651 plants demonstrating smaller increases in V_{cmax25} between 350 and 630 ppm N (39% increase)
652 than between 0 ppm N and 280 ppm N (79% increase). In contrast, nitrogen fertilization effects
653 on photosynthetic traits were absent in inoculated individuals. This pattern was also expected, as
654 inoculated plants were able to acquire sufficient nitrogen across the nitrogen availability gradient
655 to satisfy leaf-level photosynthetic demand, investing more strongly in microbial symbionts
656 under low nitrogen fertilization and shifting to nitrogen acquisition through direct uptake
657 pathways as nitrogen became more available.

658 Overall, these results indicate that leaf nitrogen-photosynthesis relationships are context-
659 dependent on nitrogen acquisition strategy, may only be constant in environments where
660 nitrogen availability limits leaf physiology, and will likely shift in response to increasing
661 atmospheric CO₂ concentrations. Terrestrial biosphere models that predict photosynthetic
662 capacity through parameterized relationships between N_{area} and V_{cmax} (Kattge *et al.*, 2009;

663 Walker *et al.*, 2014) may risk overestimating photosynthetic capacity, therefore net primary
664 productivity and the magnitude of the land carbon sink, under future novel growth environments.

665 Our results demonstrate that optimal resource allocation to photosynthetic capacity
666 defines leaf photosynthetic responses to elevated CO₂ and that these responses are not modified
667 by nitrogen availability. Current approaches for simulating photosynthetic responses to CO₂ in
668 terrestrial biosphere models with coupled carbon and nitrogen cycles often invoke patterns
669 expected from the nitrogen limitation hypothesis, where nitrogen availability diminishes with
670 time due to increasing CO₂ concentrations because whole-plant nitrogen demand continually
671 exceeds supply, depleting the pool of available nitrogen for plants to acquire and allocate to the
672 construction and maintenance of new tissues. This response causes models to simulate a
673 reduction in leaf nitrogen content and therefore photosynthetic capacity, as leaf-level
674 photosynthesis is commonly modeled as a function of positive relationships between nitrogen
675 availability, leaf nitrogen content, and photosynthetic capacity (Smith and Dukes, 2013; Rogers
676 *et al.*, 2017). Findings presented here contradict this framework, suggesting that leaf
677 photosynthetic responses to elevated CO₂ result in optimized nitrogen allocation to satisfy
678 reduced leaf nitrogen demand to build and maintain photosynthetic enzymes. Optimality models
679 that use principles from eco-evolutionary optimality theory are capable of capturing
680 photosynthetic responses to CO₂ independent of nitrogen availability (Smith and Keenan, 2020;
681 Harrison *et al.*, 2021; Stocker *et al.*, 2025), suggesting that the inclusion of such frameworks may
682 improve the accuracy by which terrestrial biosphere models simulate photosynthetic processes
683 with increasing atmospheric CO₂ concentrations.

684

685 *Limitations*

686 Previous work has highlighted that pot experiments restrict belowground rooting volume and
687 may alter plant allocation responses to environmental change (Ainsworth *et al.*, 2002; Poorter *et*
688 *al.*, 2012). In this study, the ratio of pot volume to total biomass was greater under elevated CO₂
689 and increased with increasing nitrogen fertilization such that several treatment combinations
690 exceeded values recommended to avoid growth limitation imposed by pot volume (<1 g L⁻¹;
691 Table S9; Fig. S7; Poorter *et al.*, 2012). However, there was no evidence to suggest that pot size
692 limited plant growth, as evidenced by the lack of a saturating effect of increasing fertilization on
693 total biomass, belowground carbon biomass, or root biomass under conditions where biomass:
694 pot volume ratios exceeded 1 g L⁻¹ (e.g., individuals of either inoculation status grown under
695 high fertilization and elevated CO₂). Field studies that do not restrict belowground rooting
696 volume have observed similar leaf and whole-plant responses to elevated CO₂ (Crous *et al.*,
697 2010; Lee *et al.*, 2011; Pastore *et al.*, 2019; Smith and Keenan, 2020), indicating that the pot
698 volume used in this study (6 L) was sufficient to avoid growth limitation.

699 Importantly, there are inherent limitations in using a pot experiment to make inferences
700 about how nitrogen availability modifies community- or ecosystem-level responses to elevated
701 CO₂. While we caution against using this study to make such extrapolations, a similar
702 experiment conducted under field conditions would help validate the patterns observed here
703 while providing insight into how resource competition within and across species may shape plant
704 responses to nitrogen availability and elevated CO₂.

705

706 *Conclusions*

707 Our study provides strong support for the eco-evolutionary optimality hypothesis at the leaf
708 level, where leaf photosynthetic responses to elevated CO₂ were independent of nitrogen

709 fertilization and inoculation treatment. Instead, elevated CO₂ reduced the maximum rate of
710 Rubisco carboxylation more strongly than it reduced the maximum rate of electron transport for
711 RuBP regeneration, allowing plants to achieve greater net photosynthesis rates under CO₂
712 growth conditions by approaching optimal coordination while reducing leaf nitrogen demand to
713 build and maintain photosynthetic enzymes. In contrast, at the whole-plant level, nitrogen
714 availability played a central role in regulating plant responses to elevated CO₂, consistent with
715 the nitrogen limitation hypothesis. Specifically, increases in total leaf area, total biomass, and
716 plant nitrogen under elevated CO₂ were all enhanced with increasing nitrogen fertilization.

717 While inoculation increased root nodulation under elevated CO₂, it did not significantly
718 enhance whole-plant responses to elevated CO₂, even under low nitrogen conditions where
719 plants were most strongly invested in symbiotic nitrogen-fixing bacteria. This response may have
720 been due to stronger increases in root biomass that caused plants to prioritize direct nitrogen
721 uptake pathways over symbiotic nitrogen fixation as whole-plant demand to build new tissues
722 increased, perhaps as a strategy to reduce colimitation by other nutrients, such as phosphorus.

723 Overall, plants grown under elevated CO₂ responded to increased nitrogen availability by
724 increasing the number of optimally coordinated leaves, while changes in nitrogen availability did
725 not modify the downregulation in apparent photosynthetic capacity under elevated CO₂. The
726 differential role of nitrogen availability on leaf and whole-plant responses to elevated CO₂ and
727 the dynamic leaf nitrogen-photosynthesis relationships across CO₂ and nitrogen fertilization
728 treatments suggests that terrestrial biosphere models may improve simulations of photosynthetic
729 responses to increasing atmospheric CO₂ concentrations by adopting frameworks that include
730 optimality principles.

731

732 **Supplementary data**

733 **Text S1** A continuance of the results section that describe the effects of treatment combinations
734 on mass-based leaf nitrogen content and leaf mass per unit leaf area, organ biomass, and the ratio
735 of total biomass to pot volume

736 **Table S1** Summary table containing volumes of compounds used to create modified Hoagland's
737 solutions for each soil nitrogen fertilization treatment

738 **Table S2** Summary of the daily growth chamber growing condition program

739 **Table S3** Replication scheme for each unique CO₂-by-inoculation-by-N fertilization
740 combination

741 **Table S4** Replication scheme for each unique CO₂-by-inoculation combination

742 **Table S5** Effects of treatment combinations on leaf nitrogen content and leaf mass per area

743 **Table S6** Effects of treatment combinations on dark respiration and photosynthetic nitrogen-use
744 efficiency

745 **Table S7** Effects of treatment combinations on biomass partitioning

746 **Table S8** Effects of treatment combinations on components of the carbon cost to acquire
747 nitrogen

748 **Table S9** Effects of treatment combinations on the ratio of total biomass to pot volume

749 **Figure S1** Effects of treatment combinations on mass-based leaf nitrogen content and leaf
750 biomass per unit leaf area

751 **Figure S2** Effects of CO₂ and nitrogen fertilization on area-based leaf nitrogen content, mass-
752 based leaf nitrogen content, and leaf biomass per unit leaf area

753 **Figure S3** Effects of treatment combinations on dark respiration at 25°C and photosynthetic
754 nitrogen-use efficiency at growth CO₂ concentration

755 **Figure S4** Effects of CO₂ and nitrogen fertilization on photosynthetic nitrogen-use efficiency at
756 growth CO₂ concentration

757 **Figure S5** Effects of treatment combinations on belowground biomass carbon and total nitrogen
758 biomass

759 **Figure S6** Effects of treatment combinations on root nodule biomass and root biomass

760 **Figure S7** Effects of treatment combinations on the ratio of whole-plant biomass to pot volume

761

762 **Acknowledgements**

763 This study is a contribution to the LEMONTREE (Land Ecosystem Models based On New
764 Theory, obseRvations and ExperimEnts) project, receiving support through Schmidt Sciences,
765 LLC. EAP acknowledges support from a Texas Tech University Doctoral Dissertation
766 Completion Fellowship and a Botanical Society of America Graduate Student Research Award.

767 This work was also supported by US National Science Foundation awards to NGS (DEB-
768 2045968 and DEB-2217353).

769

770 **Author contributions**

771 EAP conceptualized the study objectives and designed the experiment in collaboration with
772 NGS, collected data, conducted data analysis, and wrote the first manuscript draft. EE assisted
773 with data collection and experiment maintenance. NGS conceptualized study objectives and
774 experimental design with EAP and oversaw experiment progress. All authors provided
775 manuscript feedback and approved the manuscript in its current form for submission to *Journal*
776 *of Experimental Botany*.

777

778 **Conflict of Interest**

779 The authors declare no conflicts of interest.

780

781 **Funding**

782 US National Science Foundation (DEB-2045968 and DEB-2217353), Schmidt Sciences, LLC.

783

784 **Data Availability**

785 All R scripts, data, and metadata are available at <https://doi.org/10.5281/zenodo.12812758> (or on

786 GitHub at: https://github.com/eaperkowski/NxCO2xI_ms_data)

787

References

Adams MA, Turnbull TL, Sprent JI, Buchmann N. 2016. Legumes are different: Leaf nitrogen, photosynthesis, and water use efficiency. *Proceedings of the National Academy of Sciences of the United States of America* **113**, 4098–4103.

Ainsworth EA, Davey PA, Bernacchi CJ, et al. 2002. A meta-analysis of elevated [CO₂] effects on soybean (*Glycine max*) physiology, growth and yield. *Global Change Biology* **8**, 695–709.

Ainsworth EA, Long SP. 2005. What have we learned from 15 years of free-air CO₂ enrichment (FACE)? A meta-analytic review of the responses of photosynthesis, canopy properties and plant production to rising CO₂. *New Phytologist* **165**, 351–372.

Ainsworth EA, Rogers A. 2007. The response of photosynthesis and stomatal conductance to rising [CO₂]: mechanisms and environmental interactions. *Plant, Cell and Environment* **30**, 258–270.

Allen K, Fisher JB, Phillips RP, Powers JS, Brzostek ER. 2020. Modeling the carbon cost of plant nitrogen and phosphorus uptake across temperate and tropical forests. *Frontiers in Forests and Global Change* **3**, 1–12.

Andrews M, James EK, Sprent JI, Boddey RM, Gross E, dos Reis FB. 2011. Nitrogen fixation in legumes and actinorhizal plants in natural ecosystems: Values obtained using ^{15}N natural abundance. *Plant Ecology and Diversity* **4**, 117–130.

Arora VK, Katavouta A, Williams RG, et al. 2020. Carbon-concentration and carbon-climate feedbacks in CMIP6 models and their comparison to CMIP5 models. *Biogeosciences* **17**, 4173–4222.

Barber SA. 1962. A diffusion and mass-flow concept of soil nutrient availability. *Soil Science* **93**, 39–49.

Barnes JD, Balaguer L, Manrique E, Elvira S, Davison AW. 1992. A reappraisal of the use of DMSO for the extraction and determination of chlorophylls a and b in lichens and higher plants. *Environmental and Experimental Botany* **32**, 85–100.

Bates D, Mächler M, Bolker B, Walker S. 2015. Fitting linear mixed-effects models using lme4. *Journal of Statistical Software* **67**, 1–48.

Bazzaz FA. 1990. The response of natural ecosystems to the rising global CO₂ levels. *Annual review of ecology and systematics* **21**, 167–196.

Bernacchi CJ, Morgan PB, Ort DR, Long SP. 2005. The growth of soybean under free air [CO₂] enrichment (FACE) stimulates photosynthesis while decreasing in vivo Rubisco capacity. *Planta* **220**, 434–446.

Bernacchi CJ, Singsaas EL, Pimentel C, Portis AR, Long SP. 2001. Improved temperature response functions for models of Rubisco-limited photosynthesis. *Plant, Cell and Environment* **24**, 253–259.

Brzostek ER, Fisher JB, Phillips RP. 2014. Modeling the carbon cost of plant nitrogen acquisition: Mycorrhizal trade-offs and multipath resistance uptake improve predictions of retranslocation. *Journal of Geophysical Research: Biogeosciences* **119**, 1684–1697.

Bytnerowicz TA, Funk JL, Menge DNL, Perakis SS, Wolf AA. 2023. Leaf nitrogen affects photosynthesis and water use efficiency similarly in nitrogen-fixing and non-fixing trees. *Journal of Ecology*, 1–15.

Chen J-L, Reynolds JF, Harley PC, Tenhunen JD. 1993. Coordination theory of leaf nitrogen distribution in a canopy. *Oecologia* **93**, 63–69.

Coleman JS, McConaughay KDM, Bazzaz FA. 1993. Elevated CO₂ and plant nitrogen-use: is reduced tissue nitrogen concentration size-dependent? *Oecologia* **93**, 195–200.

Crous KY, Reich PB, Hunter MD, Ellsworth DS. 2010. Maintenance of leaf N controls the photosynthetic CO₂ response of grassland species exposed to 9 years of free-air CO₂ enrichment. *Global Change Biology* **16**, 2076–2088.

Cui E, Xia J, Luo Y. 2023. Nitrogen use strategy drives interspecific differences in plant photosynthetic CO₂ acclimation. *Global Change Biology* **29**, 3667–3677.

Curtis PS. 1996. A meta-analysis of leaf gas exchange and nitrogen in trees grown under elevated carbon dioxide. *Plant, Cell and Environment* **19**, 127–137.

Davies-Barnard T, Meyerholt J, Zaehle S, et al. 2020. Nitrogen cycling in CMIP6 land surface models: progress and limitations. *Biogeosciences* **17**, 5129–5148.

Davies-Barnard T, Zaehle S, Friedlingstein P. 2022. Assessment of the impacts of biological nitrogen fixation structural uncertainty in CMIP6 earth system models. *Biogeosciences* **19**, 3491–3503.

Dong N, Wright IJ, Chen JM, Luo X, Wang H, Keenan TF, Smith NG, Prentice IC. 2022. Rising CO₂ and warming reduce global canopy demand for nitrogen. *New Phytologist* **235**, 1692–1700.

Drake BG, González-Meler MA, Long SP. 1997. More efficient plants: a consequence of rising atmospheric CO₂? *Annual Review of Plant Biology* **48**, 609–639.

Duursma RA. 2015. Plantcophys - an R package for analysing and modelling leaf gas exchange data. *PLOS ONE* **10**, e0143346.

Evans JR. 1989. Photosynthesis and nitrogen relationships in leaves of C₃ plants. *Oecologia* **78**, 9–19.

Evans JR, Clarke VC. 2019. The nitrogen cost of photosynthesis. *Journal of Experimental Botany* **70**, 7–15.

Farquhar GD, von Caemmerer S, Berry JA. 1980. A biochemical model of photosynthetic CO₂ assimilation in leaves of C₃ species. *Planta* **149**, 78–90.

Feng Z, Rütting T, Pleijel H, Wallin G, Reich PB, Kammann CI, Newton PCD, Kobayashi K, Luo Y, Uddling J. 2015. Constraints to nitrogen acquisition of terrestrial plants under elevated CO₂. *Global Change Biology* **21**, 3152–3168.

Field CB, Mooney HA. 1986. Photosynthesis--nitrogen relationship in wild plants. On the Economy of Plant Form and Function: Proceedings of the Sixth Maria Moors Cabot Symposium, Evolutionary Constraints on Primary Productivity, Adaptive Patterns of Energy Capture in

Plants, Harvard Forest, August 1983. Cambridge [Cambridgeshire]: Cambridge University Press, c1986.

Finzi AC, Moore DJP, DeLucia EH, et al. 2006. Progressive nitrogen limitation of ecosystem processes under elevated CO₂ in a warm-temperate forest. *Ecology* **87**, 15–25.

Finzi AC, Norby RJ, Calfapietra C, et al. 2007. Increases in nitrogen uptake rather than nitrogen-use efficiency support higher rates of temperate forest productivity under elevated CO₂. *Proceedings of the National Academy of Sciences* **104**, 14014–14019.

Finzi AC, Rodgers VL. 2009. Bottom-up rather than top-down processes regulate the abundance and activity of nitrogen fixing plants in two Connecticut old-field ecosystems. *Biogeochemistry* **95**, 309–321.

Fisher JB, Sitch S, Malhi Y, Fisher RA, Huntingford C, Tan S-Y. 2010. Carbon cost of plant nitrogen acquisition: A mechanistic, globally applicable model of plant nitrogen uptake, retranslocation, and fixation. *Global Biogeochemical Cycles* **24**, 1–17.

Fox J, Weisberg S. 2019. *An R companion to applied regression*. Thousand Oaks, California: Sage.

Friel CA, Friesen ML. 2019. Legumes modulate allocation to rhizobial nitrogen fixation in response to factorial light and nitrogen manipulation. *Frontiers in Plant Science* **10**, 1316.

van Groenigen KJ, Six J, Hungate BA, De Graaff MA, Van Breemen N, Van Kessel C. 2006. Element interactions limit soil carbon storage. *Proceedings of the National Academy of Sciences of the United States of America* **103**, 6571–6574.

Gutschick VP. 1981. Evolved strategies in nitrogen acquisition by plants. *The American Naturalist* **118**, 607–637.

Harrison SP, Cramer W, Franklin O, et al. 2021. Eco-evolutionary optimality as a means to improve vegetation and land-surface models. *New Phytologist* **231**, 2125–2141.

Hoagland DR, Arnon DI. 1950. The water-culture method for growing plants without soil. California Agricultural Experiment Station: 347 **347**, 1–32.

Hungate BA, Dukes JS, Shaw MR, Luo Y, Field CB. 2003. Nitrogen and climate change. *Science* **302**, 1512–1513.

IPCC. 2021. *Climate Change 2021: The Physical Science Basis. Contribution of Working Group I to the Sixth Assessment Report of the Intergovernmental Panel on Climate Change.* (V Masson-Delmotte, P Zhai, A Pirani, *et al.*, Eds.). Cambridge, UK and New York, USA: Cambridge University Press.

Iversen CM. 2010. Digging deeper: Fine-root responses to rising atmospheric CO₂ concentration in forested ecosystems. *New Phytologist* **186**, 346–357.

Iversen CM, Ledford J, Norby RJ. 2008. CO₂ enrichment increases carbon and nitrogen input from fine roots in a deciduous forest. *New Phytologist* **179**, 837–847.

Jiang M, Calderaru S, Zhang H, et al. 2020. Low phosphorus supply constrains plant responses to elevated CO₂: A meta-analysis. *Global Change Biology* **26**, 5856–5873.

Johnson SN, Waterman JM, Hall CR. 2020. Increased insect herbivore performance under elevated CO₂ is associated with lower plant defence signalling and minimal declines in nutritional quality. *Scientific Reports* **10**, 14553.

Katabuchi M. 2015. LeafArea: An R package for rapid digital analysis of leaf area. *Ecological Research* **30**, 1073–1077.

Kattge J, Knorr W, Raddatz T, Wirth C. 2009. Quantifying photosynthetic capacity and its relationship to leaf nitrogen content for global-scale terrestrial biosphere models. *Global Change Biology* **15**, 976–991.

Kenward MG, Roger JH. 1997. Small sample inference for fixed effects from restricted maximum likelihood. *Biometrics* **53**, 983.

Kou-Giesbrecht S, Arora VK, Seiler C, et al. 2023. Evaluating nitrogen cycling in terrestrial biosphere models: a disconnect between the carbon and nitrogen cycles. *Earth System Dynamics* **14**, 767–795.

LeBauer DS, Treseder KK. 2008. Nitrogen limitation of net primary productivity in terrestrial ecosystems is globally distributed. *Ecology* **89**, 371–379.

Lee TD, Barrott SH, Reich PB. 2011. Photosynthetic responses of 13 grassland species across 11 years of free-air CO₂ enrichment is modest, consistent and independent of N supply. *Global Change Biology* **17**, 2893–2904.

Lenth R. 2019. emmeans: estimated marginal means, aka least-squares means. <https://cran.r-project.org/package=emmeans>.

Liang J, Qi X, Souza L, Luo Y. 2016. Processes regulating progressive nitrogen limitation under elevated carbon dioxide: a meta-analysis. *Biogeosciences* **13**, 2689–2699.

Lu J, Yang J, Keitel C, Yin L, Wang P, Cheng W, Dijkstra FA. 2022. Belowground carbon efficiency for nitrogen and phosphorus acquisition varies between *Lolium perenne* and *Trifolium repens* and depends on phosphorus fertilization. *Frontiers in Plant Science* **13**, 1–9.

Luo Y, Currie WS, Dukes JS, et al. 2004. Progressive nitrogen limitation of ecosystem responses to rising atmospheric carbon dioxide. *BioScience* **54**, 731–739.

Luo Y, Field CB, Mooney HA. 1994. Predicting responses of photosynthesis and root fraction to elevated [CO₂]: interactions among carbon, nitrogen, and growth. *Plant, Cell & Environment* **17**, 1195–1204.

Luo X, Keenan TF, Chen JM, et al. 2021. Global variation in the fraction of leaf nitrogen allocated to photosynthesis. *Nature Communications* **12**, 4866.

Maire V, Martre P, Kattge J, Gastal F, Esser G, Fontaine S, Soussana J-F. 2012. The coordination of leaf photosynthesis links C and N fluxes in C₃ plant species. *PLoS ONE* **7**, e38345.

Makino A, Harada M, Sato T, Nakano H, Mae T. 1997. Growth and N allocation in rice plants under CO₂ enrichment. *Plant Physiology* **115**, 199–203.

McCulloch LA, Porder S. 2021. Light fuels while nitrogen suppresses symbiotic nitrogen fixation hotspots in neotropical canopy gap seedlings. *New Phytologist* **231**, 1734–1745.

Medlyn BE, Badeck FW, De Pury DGG, et al. 1999. Effects of elevated [CO₂] on photosynthesis in European forest species: A meta-analysis of model parameters. *Plant, Cell and Environment* **22**, 1475–1495.

Meyerholt J, Sickel K, Zaehle S. 2020. Ensemble projections elucidate effects of uncertainty in terrestrial nitrogen limitation on future carbon uptake. *Global Change Biology* **26**, 3978–3996.

Moore DJP, Aref S, Ho RM, Pippen JS, Hamilton JG, De Lucia EH. 2006. Annual basal area increment and growth duration of *Pinus taeda* in response to eight years of free-air carbon dioxide enrichment. *Global Change Biology* **12**, 1367–1377.

Nakano H, Makino A, Mae T. 1997. The effect of elevated partial pressures of CO₂ on the relationship between photosynthetic capacity and N content in rice leaves. *Plant Physiology* **115**, 191–198.

- Nie M, Lu M, Bell J, Raut S, Pendall E.** 2013. Altered root traits due to elevated CO₂: A meta-analysis. *Global Ecology and Biogeography* **22**, 1095–1105.
- Niinemets Ü, Tenhunen JD.** 1997. A model separating leaf structural and physiological effects on carbon gain along light gradients for the shade-tolerant species *Acer saccharum*. *Plant, Cell and Environment* **20**, 845–866.
- Norby RJ, Warren JM, Iversen CM, Medlyn BE, McMurtrie RE.** 2010. CO₂ enhancement of forest productivity constrained by limited nitrogen availability. *Proceedings of the National Academy of Sciences* **107**, 19368–19373.
- Nowak RS, Ellsworth DS, Smith SD.** 2004. Functional responses of plants to elevated atmospheric CO₂ - Do photosynthetic and productivity data from FACE experiments support early predictions? *New Phytologist* **162**, 253–280.
- Onoda Y, Wright IJ, Evans JR, Hikosaka K, Kitajima K, Niinemets Ü, Poorter H, Tosens T, Westoby M.** 2017. Physiological and structural tradeoffs underlying the leaf economics spectrum. *New Phytologist* **214**, 1447–1463.
- Pastore MA, Lee TD, Hobbie SE, Reich PB.** 2019. Strong photosynthetic acclimation and enhanced water-use efficiency in grassland functional groups persist over 21 years of CO₂ enrichment, independent of nitrogen supply. *Global Change Biology* **25**, 3031–3044.
- Peng Y, Prentice IC, Bloomfield KJ, Campioli M, Guo Z, Sun Y, Tian D, Wang X, Vicca S, Stocker BD.** 2023. Global terrestrial nitrogen uptake and nitrogen use efficiency. *Journal of Ecology*, 1–18.
- Perkowski EA, Terrones J, German HL, Smith NG.** 2024. Symbiotic nitrogen fixation reduces belowground biomass carbon costs of nitrogen acquisition under low, but not high, nitrogen availability. *AoB PLANTS* **16**, 1–22.

Perkowski EA, Waring EF, Smith NG. 2021. Root mass carbon costs to acquire nitrogen are determined by nitrogen and light availability in two species with different nitrogen acquisition strategies. *Journal of Experimental Botany* **72**, 5766–5776.

Poorter H, Böhler J, Van Dusschoten D, Climent J, Postma JA. 2012. Pot size matters: A meta-analysis of the effects of rooting volume on plant growth. *Functional Plant Biology* **39**, 839–850.

Poorter H, Knopf O, Wright IJ, Temme AA, Hogewoning SW, Graf A, Cernusak LA, Pons TL. 2022. A meta-analysis of responses of C₃ plants to atmospheric CO₂: dose–response curves for 85 traits ranging from the molecular to the whole-plant level. *New Phytologist* **233**, 1560–1596.

Prentice IC, Dong N, Gleason SM, Maire V, Wright IJ. 2014. Balancing the costs of carbon gain and water transport: testing a new theoretical framework for plant functional ecology. *Ecology Letters* **17**, 82–91.

Prentice IC, Liang X, Medlyn BE, Wang Y-P. 2015. Reliable, robust and realistic: The three R's of next-generation land-surface modelling. *Atmospheric Chemistry and Physics* **15**, 5987–6005.

R Core Team. 2021. R: A language and environment for statistical computing. <https://www.r-project.org/>.

Rastetter EB, Vitousek PM, Field CB, Shaver GR, Herbert D, Ågren GI. 2001. Resource optimization and symbiotic nitrogen fixation. *Ecosystems* **4**, 369–388.

Reich PB, Hobbie SE, Lee TD, Ellsworth DS, West JB, Tilman D, Knops JMH, Naeem S, Trost J. 2006. Nitrogen limitation constrains sustainability of ecosystem response to CO₂. *Nature* **440**, 922–925.

- Rogers A, Ainsworth EA, Leakey ADB.** 2009. Will elevated carbon dioxide concentration amplify the benefits of nitrogen fixation in legumes? *Plant Physiology* **151**, 1009–1016.
- Rogers A, Medlyn BE, Dukes JS, et al.** 2017. A roadmap for improving the representation of photosynthesis in Earth system models. *New Phytologist* **213**, 22–42.
- Saathoff AJ, Welles J.** 2021. Gas exchange measurements in the unsteady state. *Plant Cell and Environment* **44**, 3509–3523.
- Sage RF.** 1994. Acclimation of photosynthesis to increasing atmospheric CO₂: The gas exchange perspective. *Photosynthesis Research* **39**, 351–368.
- Schneider CA, Rasband WS, Eliceiri KW.** 2012. NIH Image to ImageJ: 25 years of image analysis. *Nature Methods* **9**, 671–675.
- Sigurdsson BD, Medhurst JL, Wallin G, Eggertsson O, Linder S.** 2013. Growth of mature boreal Norway spruce was not affected by elevated [CO₂] and/or air temperature unless nutrient availability was improved. *Tree Physiology* **33**, 1192–1205.
- Smith NG, Dukes JS.** 2013. Plant respiration and photosynthesis in global-scale models: incorporating acclimation to temperature and CO₂. *Global Change Biology* **19**, 45–63.
- Smith NG, Keenan TF.** 2020. Mechanisms underlying leaf photosynthetic acclimation to warming and elevated CO₂ as inferred from least-cost optimality theory. *Global Change Biology* **26**, 5202–5216.
- Smith NG, Keenan TF, Prentice IC, et al.** 2019. Global photosynthetic capacity is optimized to the environment. *Ecology Letters* **22**, 506–517.
- Smith SE, Read DJ.** 2008. *Mycorrhizal Symbiosis*.

Smith NG, Zhu Q, Keenan TF, Riley WJ. 2024. Acclimation of photosynthesis to CO₂ increases ecosystem carbon storage due to leaf nitrogen savings. *Global Change Biology* **30**, 1–10.

Stocker BD, Dong N, Perkowski EA, et al. 2025. Empirical evidence and theoretical understanding of ecosystem carbon and nitrogen cycle interactions. *New Phytologist* **245**, 49–68.

Taylor BN, Menge DNL. 2018. Light regulates tropical symbiotic nitrogen fixation more strongly than soil nitrogen. *Nature Plants* **4**, 655–661.

Tejera-Nieves M, Seong DY, Reist L, Walker BJ. 2024. The Dynamic Assimilation Technique measures photosynthetic CO₂ response curves with similar fidelity to steady-state approaches in half the time. *Journal of Experimental Botany* **75**, 2819–2828.

Terrer C, Vicca S, Hungate BA, Phillips RP, Prentice IC. 2016. Mycorrhizal association as a primary control of the CO₂ fertilization effect. *Science* **353**, 72–74.

Terrer C, Vicca S, Stocker BD, Hungate BA, Phillips RP, Reich PB, Finzi AC, Prentice IC. 2018. Ecosystem responses to elevated CO₂ governed by plant–soil interactions and the cost of nitrogen acquisition. *New Phytologist* **217**, 507–522.

Vitousek PM, Howarth RW. 1991. Nitrogen limitation on land and in the sea: How can it occur? *Biogeochemistry* **13**, 87–115.

Walker AP, Beckerman AP, Gu L, Kattge J, Cernusak LA, Domingues TF, Scales JC, Wohlfahrt G, Wullschleger SD, Woodward FI. 2014. The relationship of leaf photosynthetic traits - V_{cmax} and J_{max} - to leaf nitrogen, leaf phosphorus, and specific leaf area: a meta-analysis and modeling study. *Ecology and Evolution* **4**, 3218–3235.

Wang H, Prentice IC, Keenan TF, Davis TW, Wright IJ, Cornwell WK, Evans BJ, Peng C. 2017. Towards a universal model for carbon dioxide uptake by plants. *Nature Plants* **3**, 734–741.

- Waring EF, Perkowski EA, Smith NG.** 2023. Soil nitrogen fertilization reduces relative leaf nitrogen allocation to photosynthesis. *Journal of Experimental Botany* **74**, 5166–5180.
- Wellburn AR.** 1994. The spectral determination of chlorophylls a and b, as well as total carotenoids, using various solvents with spectrophotometers of different resolution. *Journal of Plant Physiology* **144**, 307–313.
- Wieder WR, Cleveland CC, Smith WK, Todd-Brown K.** 2015. Future productivity and carbon storage limited by terrestrial nutrient availability. *Nature Geoscience* **8**, 441–444.
- Wright IJ, Reich PB, Westoby M.** 2003. Least-cost input mixtures of water and nitrogen for photosynthesis. *The American Naturalist* **161**, 98–111.
- Zavala JA, Nabity PD, DeLucia EH.** 2013. An Emerging Understanding of Mechanisms Governing Insect Herbivory Under Elevated CO₂. *Annual Review of Entomology* **58**, 79–97.

Table 1 Effects of CO₂ concentration, inoculation, and nitrogen fertilization on area-based leaf nitrogen content and chlorophyll content*

		<i>N</i> _{area}		<i>Chl</i> _{area}	
	df	χ^2	<i>p</i>	χ^2	<i>p</i>
CO ₂	1	155.908	<0.001	62.056	<0.001
Inoculation (I)	1	86.029	<0.001	133.828	<0.001
N fertilization (N)	1	316.408	<0.001	156.659	<0.001
CO ₂ × I	1	4.729	0.030	1.647	0.199
CO ₂ × N	1	5.723	0.017	2.780	0.095
I × N	1	43.381	<0.001	73.494	<0.001
CO ₂ × I × N	1	0.489	0.484	2.123	0.145

*Significance determined using Type II Wald χ^2 tests ($\alpha=0.05$). *P*-values less than 0.05 are in bold. Key: df=degrees of freedom, χ^2 =Wald chi-square test statistic, *N*_{area}=leaf nitrogen content per unit leaf area (gN m⁻²), *Chl*_{area}=chlorophyll content per unit leaf area (mmol m⁻²)

Table 2 Effects of CO₂ concentration, inoculation, and nitrogen fertilization on leaf gas exchange*

	<i>A</i> _{net,420}			<i>A</i> _{net,gc}			<i>V</i> _{cmax25}			<i>J</i> _{max25}			<i>J</i> _{max25:<i>V</i>_{cmax25}}	
	df	χ^2	p	χ^2	p	χ^2	p	χ^2	p	χ^2	p	χ^2	p	
CO ₂	1	15.747	<0.001	52.716	<0.001	18.039	<0.001	6.042	0.014	92.010	<0.001			
Inoculation (I)	1	77.137	<0.001	83.008	<0.001	98.579	<0.001	85.064	<0.001	27.768	<0.001			
N fertilization (N)	1	11.986	<0.001	14.658	<0.001	37.053	<0.001	25.356	<0.001	28.147	<0.001			
CO ₂ × I	1	1.032	0.310	5.634	0.018	0.065	0.799	0.667	0.414	2.916	0.088			
CO ₂ × N	1	1.998	0.158	0.135	0.713	1.758	0.185	0.742	0.389	3.210	0.073			
I × N	1	46.800	<0.001	50.774	<0.001	60.394	<0.001	57.41	<0.001	9.607	0.002			
CO ₂ × I × N	1	0.002	0.964	1.332	0.248	0.748	0.387	0.377	0.539	1.102	0.294			

*Significance determined using Type II Wald χ^2 tests ($\alpha=0.05$). P-values less than 0.05 are in bold. Key: df=degrees of freedom,

χ^2 =Wald chi-square test statistic, $A_{\text{net},420}$ =net photosynthesis rate at 420 $\mu\text{mol mol}^{-1}$ CO₂ ($\mu\text{mol m}^{-2} \text{s}^{-1}$), $A_{\text{net,gc}}$ =net photosynthesis rate

at under growth CO₂ condition ($\mu\text{mol m}^{-2} \text{s}^{-1}$), V_{cmax25} =apparent maximum rate of Rubisco carboxylation at 25°C ($\mu\text{mol m}^{-2} \text{s}^{-1}$),

J_{max25} =apparent maximum rate of electron transport for RuBP regeneration at 25°C ($\mu\text{mol m}^{-2} \text{s}^{-1}$), $J_{\text{max25}}:V_{\text{cmax25}}$ =ratio of J_{max25} to

V_{cmax25} (unitless)

Table 3 Effects of CO₂ concentration, inoculation, and nitrogen fertilization on total leaf area, total biomass, carbon costs to acquire nitrogen, and plant investment toward symbiotic nitrogen fixation*

	df	Total leaf area χ^2	p	Total biomass ^b χ^2	p	Root:shoot ratio ^a χ^2	p
CO ₂	1	69.291	<0.001	131.477	<0.001	4.892	0.027
Inoculation (I)	1	35.715	<0.001	34.264	<0.001	9.790	0.002
N fertilization (N)	1	274.199	<0.001	269.046	<0.001	50.742	<0.001
CO ₂ × I	1	2.064	0.151	0.518	0.472	10.467	0.001
CO ₂ × N	1	18.655	<0.001	16.877	<0.001	0.012	0.914
I × N	1	10.804	0.001	15.779	<0.001	3.802	0.051
CO ₂ × I × N	1	<0.001	0.990	0.023	0.880	0.417	0.519

	Carbon cost to acquire nitrogen ^a		Nodule biomass: root biomass	
	χ^2	p	χ^2	p
CO ₂	76.462	<0.001	0.010	0.921
Inoculation (I)	70.846	<0.001	902.063	<0.001
N fertilization (N)	74.961	<0.001	254.741	<0.001
CO ₂ × I	33.329	<0.001	21.632	<0.001
CO ₂ × N	1.889	0.169	1.590	0.207
I × N	26.719	<0.001	132.463	<0.001
CO ₂ × I × N	6.860	0.009	2.481	0.115

*Significance determined using Type II Wald χ^2 tests ($\alpha=0.05$). P-values less than 0.05 are in bold and p-values where $0.05 < p < 0.1$ are in italic font. Key: ^a=variable was natural log transformed before model fitting, ^b=variable was square root transformed before model fitting, df=degrees of freedom, χ^2 =Wald chi-square test statistic, total leaf area (cm²), total biomass (g), the ratio of root biomass to shoot biomass (unitless), belowground biomass carbon cost to acquire nitrogen (gC gN⁻¹), the ratio of root nodule biomass to root biomass (unitless)

Figure Legends

Figure 1 Effects of CO₂ concentration, inoculation, and nitrogen fertilization on leaf nitrogen per unit leaf area (a) and chlorophyll content per unit leaf area (b). Nitrogen fertilization is on the x-axis in both panels. Red shaded points and trendlines indicate plants grown under elevated CO₂, while blue shaded points and trendlines indicate plants grown under ambient CO₂. Light blue and light red circular points and trendlines indicate measurements collected from uninoculated plants, while dark blue and dark red triangular points indicate measurements collected from inoculated plants. Solid trendlines indicate regression slopes that are different from zero ($p<0.05$), while dashed trendlines indicate slopes that are not distinguishable from zero ($p>0.05$). Error ribbons of each trendline represent the upper and lower 95% confidence intervals.

Figure 2 Effects of CO₂, inoculation, and nitrogen fertilization on net photosynthesis measured under growth CO₂ concentration (a), the apparent maximum rate of Rubisco carboxylation at 25°C (b), the apparent maximum rate of electron transport for RuBP regeneration at 25°C (c), and the ratio of the apparent maximum rate of electron transport for RuBP regeneration to the apparent maximum rate of Rubisco carboxylation (d). Nitrogen fertilization is on the x-axis in all panels. Red shaded points and trendlines indicate plants grown under elevated CO₂, while blue shaded points and trendlines indicate plants grown under ambient CO₂. Light blue and light red circular points and trendlines indicate measurements collected from uninoculated plants, while dark blue and dark red triangular points indicate measurements collected from inoculated plants. Solid trendlines indicate regression slopes that are different from zero ($p<0.05$), while dashed trendlines indicate slopes that are not distinguishable from zero ($p>0.05$). Error ribbons of each trendline represent the upper and lower 95% confidence intervals.

Figure 3 Effects of CO₂, nitrogen fertilization, and inoculation on total leaf area (a), total biomass (b), the ratio of root biomass to shoot biomass (c), and belowground carbon cost to acquire nitrogen (d). Nitrogen fertilization is on the x-axis in all panels. Red shaded points and trendlines indicate plants grown under elevated CO₂, while blue shaded points and trendlines indicate plants grown under ambient CO₂. Light blue and light red circular points and trendlines indicate measurements collected from uninoculated plants, while dark blue and dark red triangular points indicate measurements collected from inoculated plants. Solid trendlines indicate regression slopes that are different from zero ($p<0.05$), while dashed trendlines indicate slopes that are not distinguishable from zero ($p>0.05$). Error ribbons of each trendline represent the upper and lower 95% confidence intervals.

Figure 4 Effects of CO₂, nitrogen fertilization, and inoculation on the ratio of root nodule biomass to root biomass. Nitrogen fertilization is on the x-axis. Red shaded points and trendlines indicate plants grown under elevated CO₂, while blue shaded points and trendlines indicate plants grown under ambient CO₂. Light blue and light red circular points and trendlines indicate measurements collected from uninoculated plants, while dark blue and dark red triangular points indicate measurements collected from inoculated plants. Solid trendlines indicate regression slopes that are different from zero ($p<0.05$), while dashed trendlines indicate slopes that are not distinguishable from zero ($p>0.05$). Error ribbons of each trendline represent the upper and lower 95% confidence intervals.

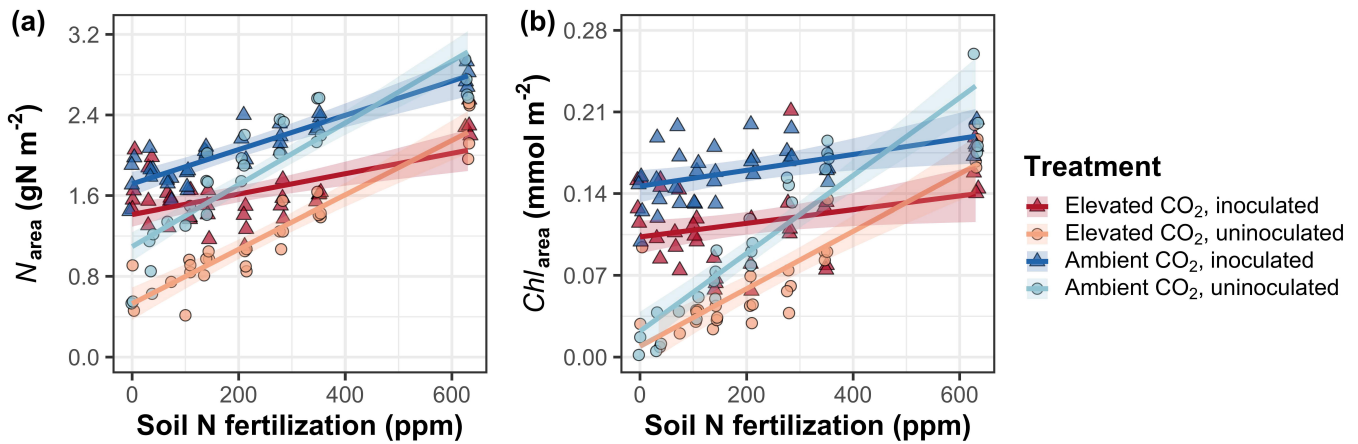


Figure 1. Effects of CO_2 concentration, inoculation, and nitrogen fertilization on leaf nitrogen per unit leaf area (a) and chlorophyll content per unit leaf area (b). Nitrogen fertilization is on the x-axis in both panels. Red shaded points and trendlines indicate plants grown under elevated CO_2 , while blue shaded points and trendlines indicate plants grown under ambient CO_2 . Light blue and light red circular points and trendlines indicate measurements collected from uninoculated plants, while dark blue and dark red triangular points indicate measurements collected from inoculated plants. Solid trendlines indicate regression slopes that are different from zero ($p < 0.05$), while dashed trendlines indicate slopes that are not distinguishable from zero ($p > 0.05$). Error ribbons of each trendline represent the upper and lower 95% confidence intervals

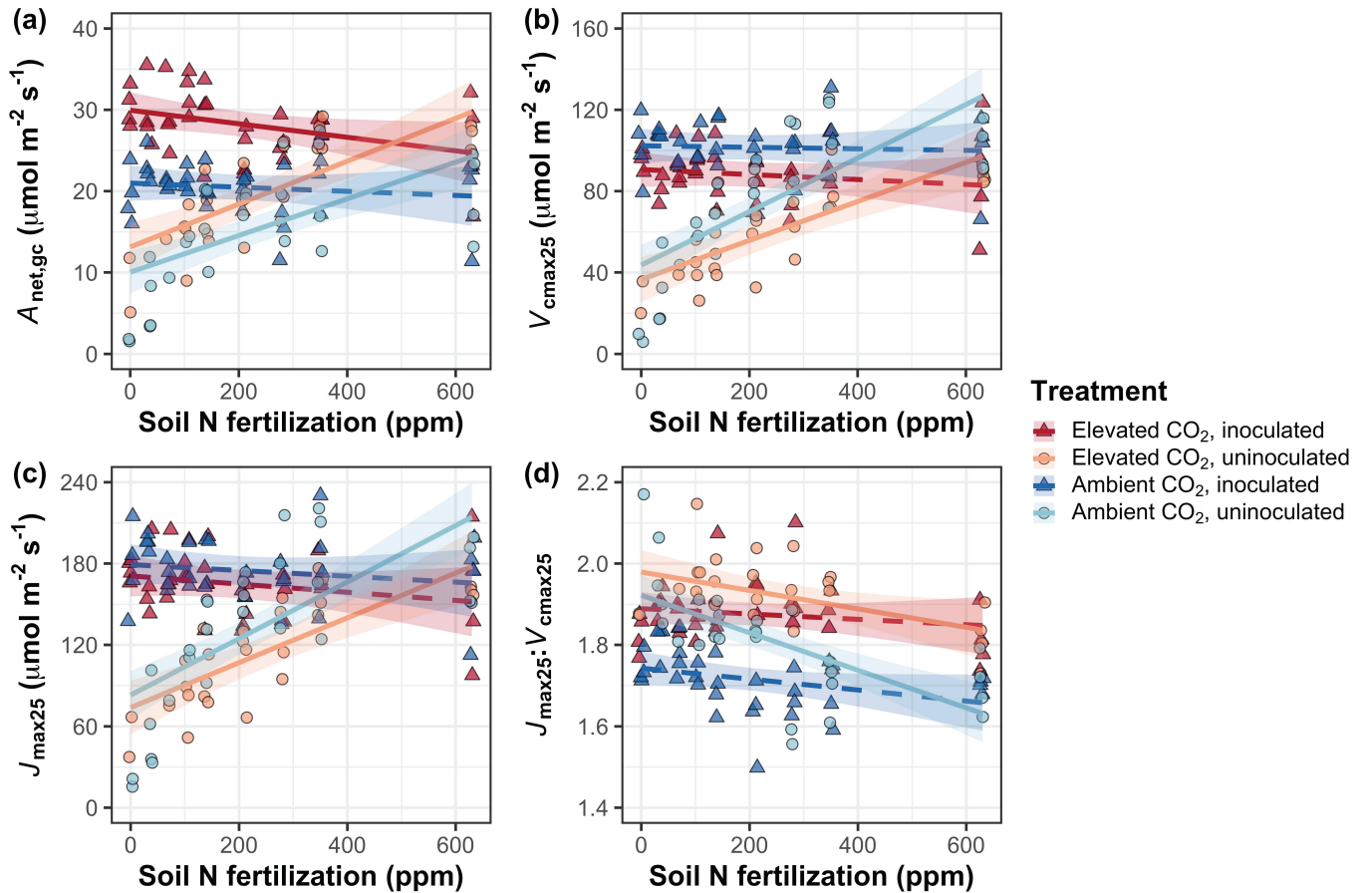


Figure 2. Effects of CO₂ concentration, inoculation, and nitrogen fertilization on net photosynthesis measured under growth CO₂ concentration (a), the apparent maximum rate of Rubisco carboxylation at 25°C (b), the apparent maximum rate of electron transport for RuBP regeneration at 25°C (c), and the ratio of the apparent maximum rate of electron transport for RuBP regeneration to the apparent maximum rate of Rubisco carboxylation (d). Nitrogen fertilization is on the x-axis in all panels. Red shaded points and trendlines indicate plants grown under elevated CO₂, while blue shaded points and trendlines indicate plants grown under ambient CO₂. Light blue and light red circular points and trendlines indicate measurements collected from uninoculated plants, while dark blue and dark red triangular points indicate measurements collected from inoculated plants. Solid trendlines indicate regression slopes that are different from zero ($p < 0.05$), while dashed trendlines indicate slopes that are not distinguishable from zero ($p > 0.05$). Error ribbons of each trendline represent the upper and lower 95% confidence intervals.

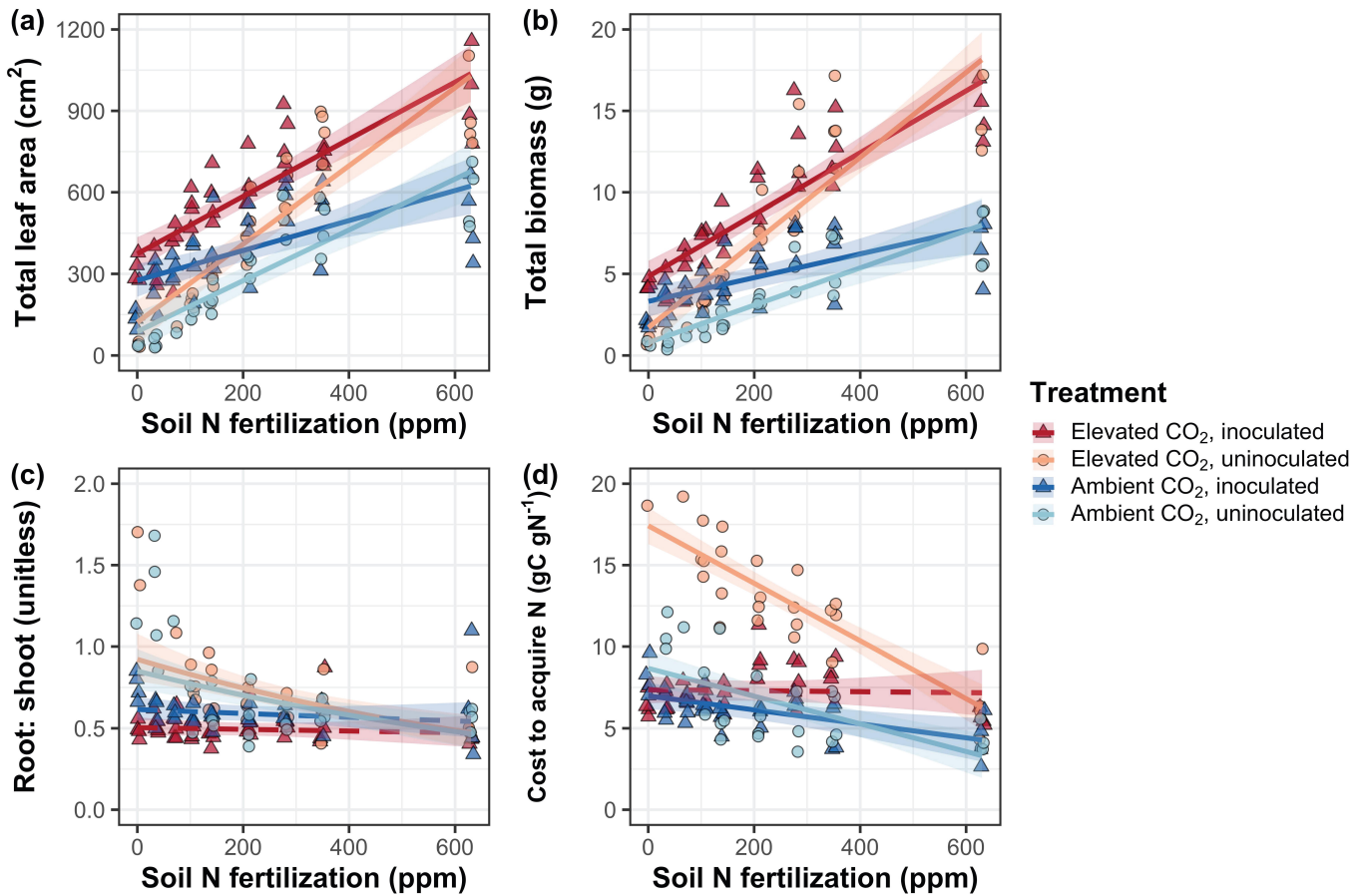


Figure 3. Effects of CO₂ concentration, inoculation, and nitrogen fertilization on total leaf area (a), total biomass (b), the ratio of root biomass to shoot biomass (c), and belowground carbon cost to acquire nitrogen (d). Nitrogen fertilization is on the x-axis in all panels. Red shaded points and trendlines indicate plants grown under elevated CO₂, while blue shaded points and trendlines indicate plants grown under ambient CO₂. Light blue and light red circular points and trendlines indicate measurements collected from uninoculated plants, while dark blue and dark red triangular points indicate measurements collected from inoculated plants. Solid trendlines indicate regression slopes that are different from zero ($p < 0.05$), while dashed trendlines indicate slopes that are not distinguishable from zero ($p > 0.05$). Error ribbons of each trendline represent the upper and lower 95% confidence intervals.

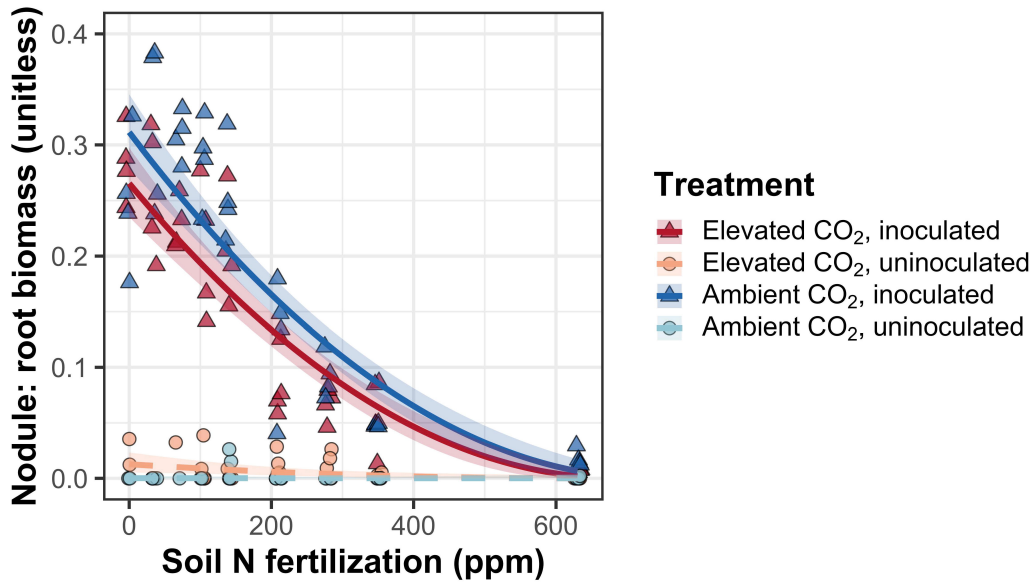


Figure 4. Effects of CO₂ concentration, inoculation, and nitrogen fertilization on the ratio of root nodule biomass to root biomass. Nitrogen fertilization is on the x-axis. Red shaded points and trendlines indicate plants grown under elevated CO₂, while blue shaded points and trendlines indicate plants grown under ambient CO₂. Light blue and light red circular points and trendlines indicate measurements collected from uninoculated plants, while dark blue and dark red triangular points indicate measurements collected from inoculated plants. Solid trendlines indicate regression slopes that are different from zero ($p<0.05$), while dashed trendlines indicate slopes that are not distinguishable from zero ($p>0.05$). Error ribbons of each trendline represent the upper and lower 95% confidence intervals.